CERN Science Gateway
designed by
Renzo Piano Building Workshop

CERN Science Gateway
Inauguration
(7 October 2023)

Update on Superconducting Magnets & Devices Development at CERN

prepared by A. Devred

CERN/TE-HDO

with support from a large number of colleagues from CERN/TE-MSC, CERN/EN-MME and CERN/TE-VSC

University of Genova
Genova, Italy

4 June 2024

Foreword

- **Warm thanks** for the opportunity of this seminar.
- In the next hour, I will try to present selected activities of the **Magnets, Superconductors and Cryostats Group at CERN** over the past few years.
- The selection omits all work related to **normal conducting magnets,** which are so critical to the operation and upgrade of the CERN accelerator complex; il also omits all the work done on **Nb-Ti magnets for HL-LHC**, although these magnets do push the limits of Nb-Ti technology.
- The development of **Nb_3Sn HL-LHC magnets** was initiated in the USA: **Fermilab for 11 T dipole magnets, LARP and AUP for MQXF quadrupole magnets;** I will not go into history and will concentrate on **recent CERN activities.**
- Of course, none of this would have been possible without the efforts of **L. Rossi** to launch the **HL-LHC project and associated collaborations** (circa 2010) and the **great contributions from the US "pioneers"** to Nb_3Sn accelerator magnet development, in particular at **LBNL and Fermilab.**
- **A large number of people from various Groups** (at CERN and outside) have been involved in the work reported here; I will try to cite them in the slides as I go along and I sincerely hope I did not miss anybody.

Table of Content

HL-LHC Project

Overview

Superconducting Link Systems

Nb_3Sn Dipole and Quadrupole Magnets

High-Luminosity LHC Project

Courtesy of L. Rossi (formerly CERN)

- The 27-km-circumference **Large Hadron Collider (LHC)** is presently the crown Jewell of the CERN accelerator complex.
- It is now operating reliably at a record energy of **6.8 TeV per beam,** corresponding to a **bore/ peak field of 8.06/8.45 T** in the dipole magnets (Nb–Ti @1.9 K).
- The next step for CERN is **the High Luminosity upgrade of the LHC (HL-LHC),** which includes several **technical innovations** aimed at **boosting performances and efficiency.**
- **HL-LHC installation** is foreseen in **2026-2028.**

First use of ~100-m-long, **MgB_2 superconducting links** to power magnet strings in Interaction Regions

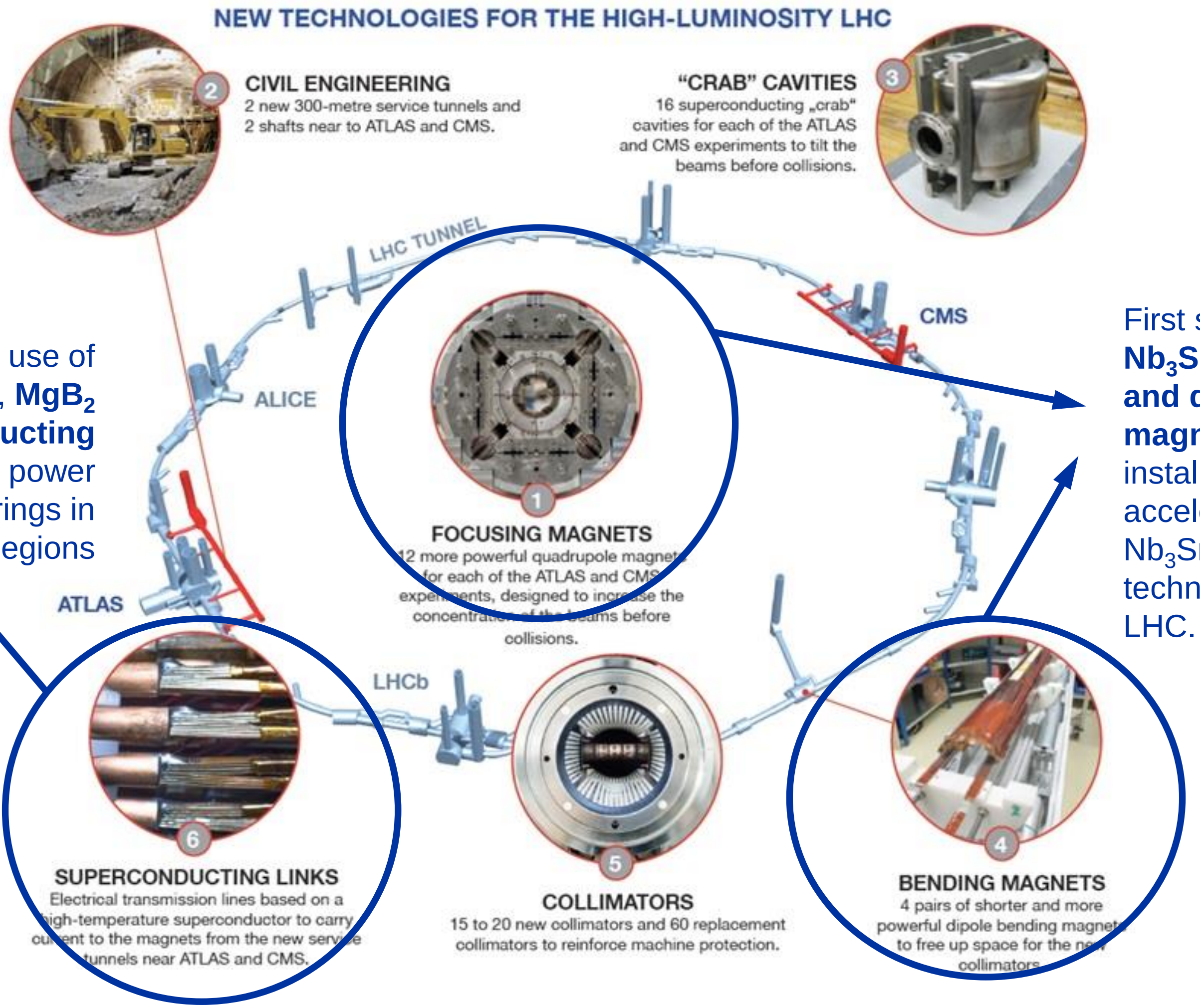

First sets of **Nb_3Sn dipole and quadrupole magnets** to be installed in an accelerator; Nb_3Sn is an enabling technology for HL-LHC.

HL-LHC Cold Powering System (1/4)

Courtesy of A. Ballarino
(CERN TE-MSC)

- **Innovative systems** supplying current to all HL-LHC Interaction Region **magnets and correctors.**
- Several circuits in **parallel,** with lengths in excess of **100 m** (including a vertical section of **~10 m).**

Implementation of HL-LHC sc links to connect power converters in the new HL-LHC gallery to the IR magnets in the LHC tunnel

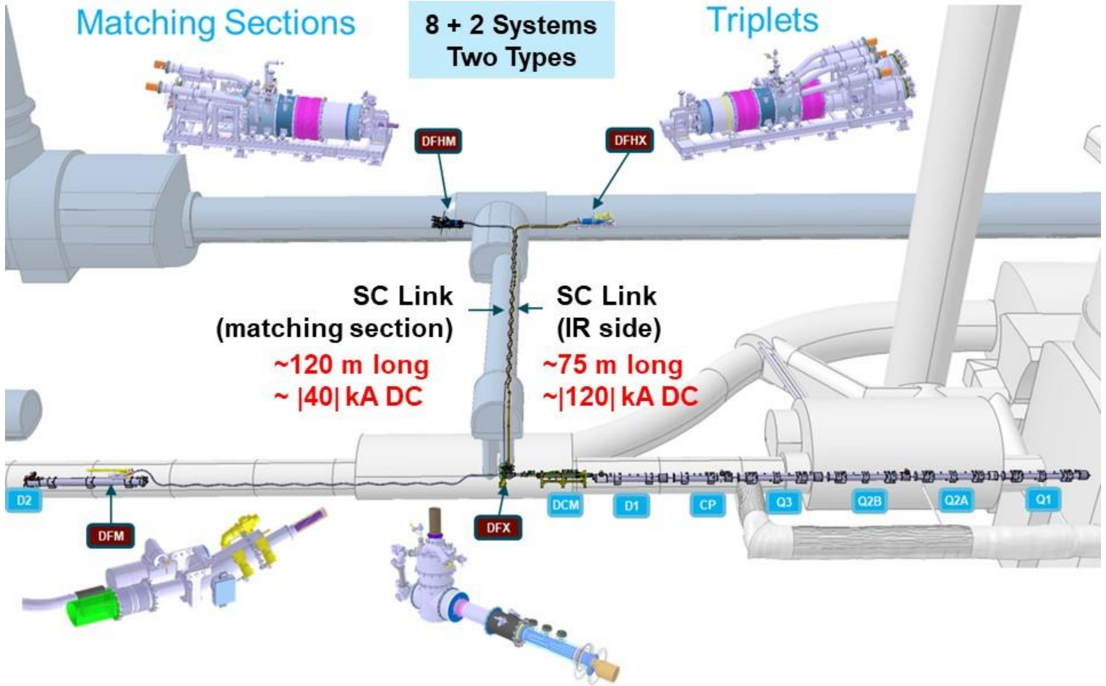

18 kA @ 25 K,
~24 mm ∅

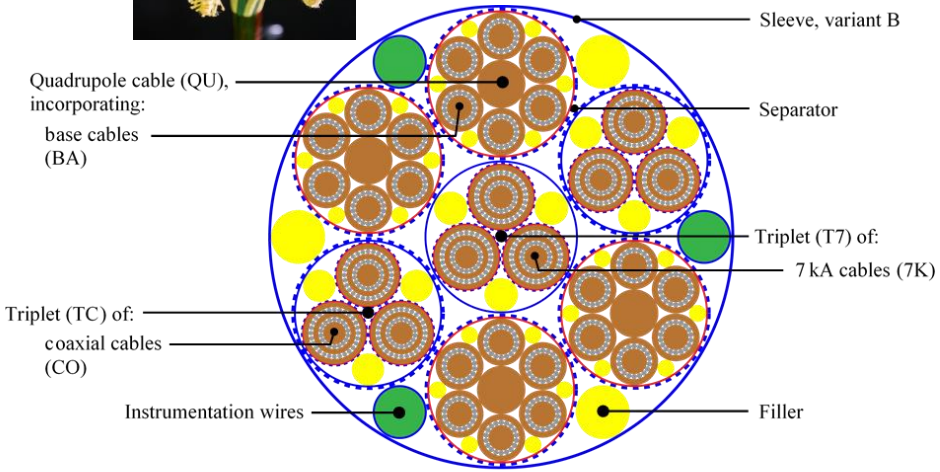

Layout of HL-LHC superconducting link cable for inner triplet side

- **Multi-stage MgB_2 cable** cooled by **forced flow of GHe** at temperatures in the **4.5-20 K** range, and designed to carry up to **~120 kA @25 K.**
- **First large-scale production of MgB_2 wires** (scope: 280 + 1050 km).

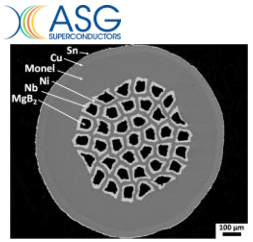

HL-LHC Cold Powering System (2/4)

Courtesy of A. Ballarino
(CERN TE-MSC)

- **Cabling** is carried out on **reacted MgB_2 wires** and requires **special equipment and care.**

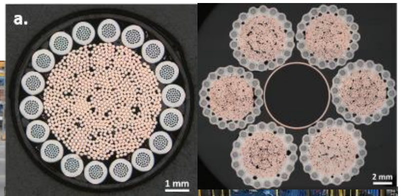

December 2019
Tratos Cavi

Pre-series DFX
(March 2022)

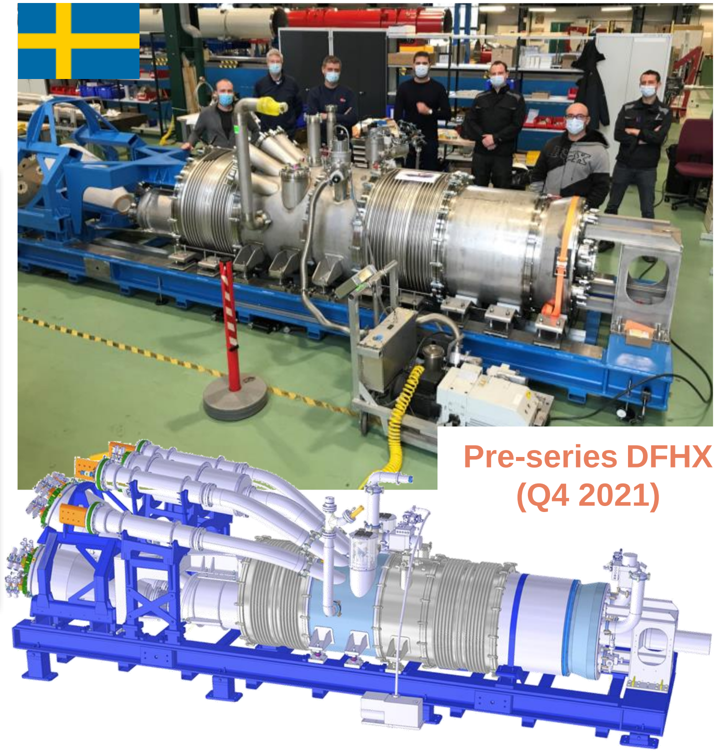

Pre-series DFHX
(Q4 2021)

- The system includes complex **feed boxes** at both ends of the link **(DFX** on the cold side, in collaboration with **Southampton University,** and **DFH** on the warm side, in collaboration with **Uppsala University).**

HL-LHC Cold Powering System (3/4)

Courtesy of A. Ballarino
(CERN TE-MSC)

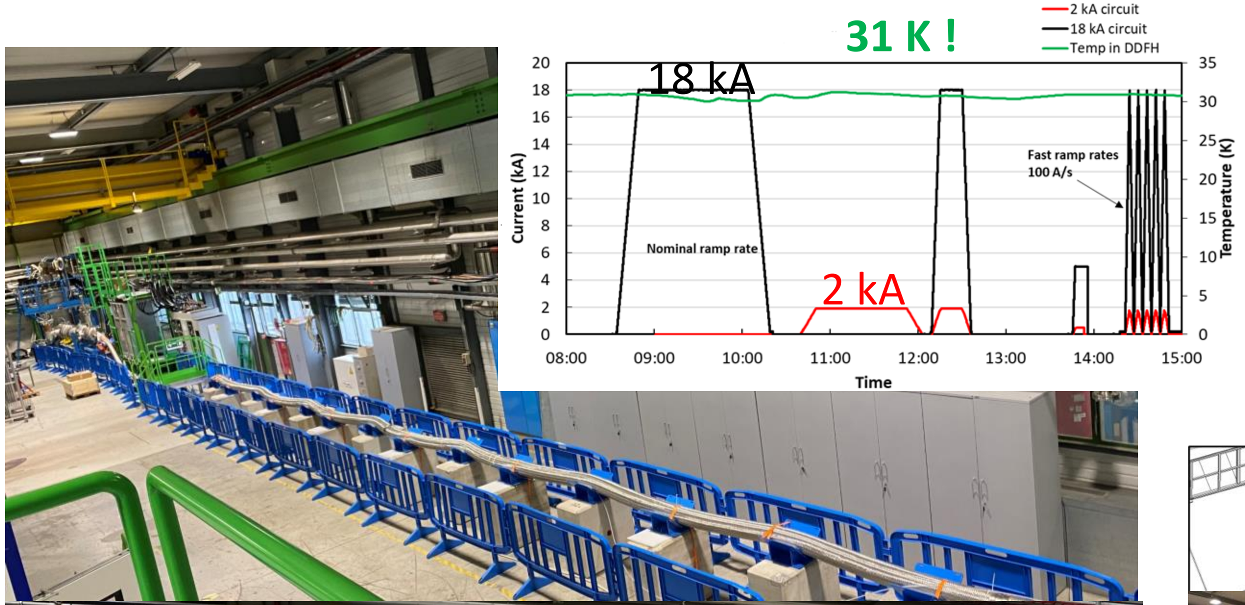

- Design, manufacturing and assembly processes of components have been **qualified through a successful series of three demonstrators.**
- Next step is a **full-size prototype system test,** incorporating **all components** and a **topology** similar to the one foreseen in the tunnel and gallery.

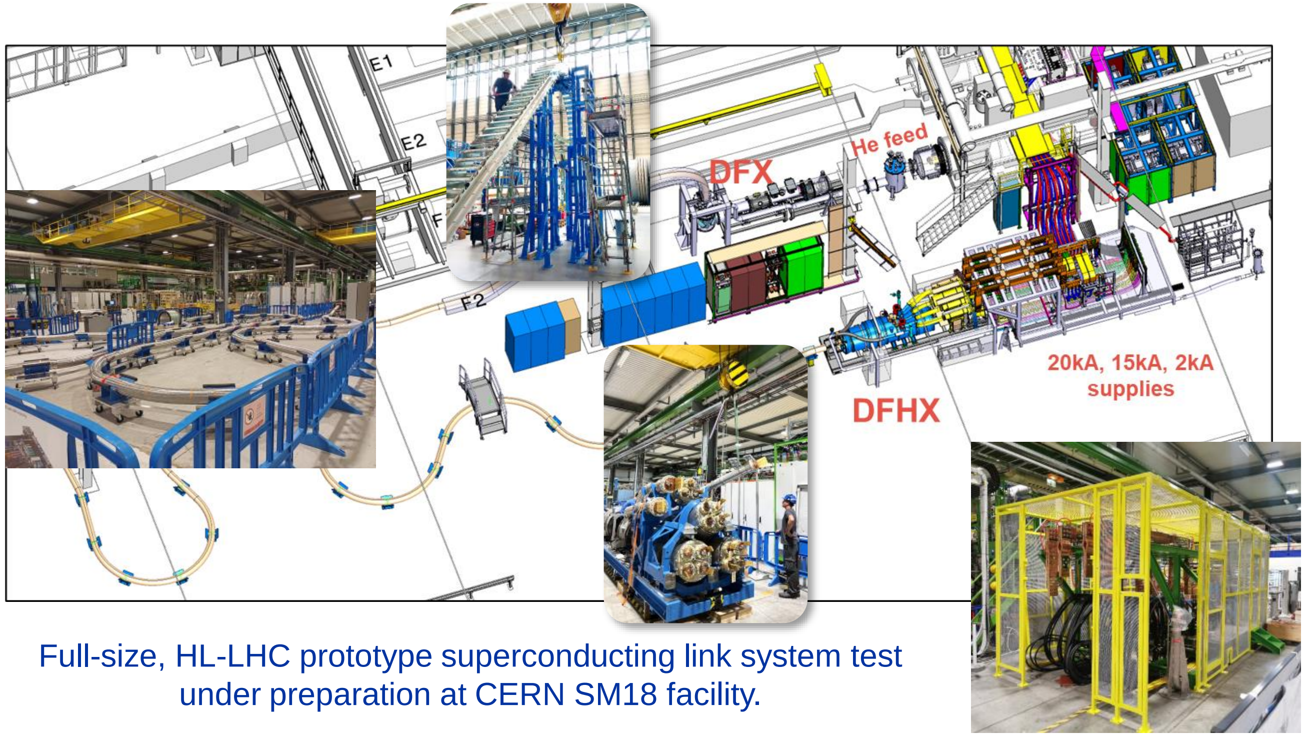

Full-size, HL-LHC prototype superconducting link system test under preparation at CERN SM18 facility.

HL-LHC Cold Powering System (4/4)

Prepared with A. Ballarino
(CERN TE-MSC)

- **Mechanical assembly** of superconducting link prototype system was completed in **December 2023;** pressure & leak test were successfully carried out in **January 2024.**

- First **series system** successfully tested at CERN in **March 2024;** electrical and cryogenic results **in line with specifications**; transferred up to **94 kA in DC mode; minimum flow of 5 g/s** gives a temperature at **MgB_2-HTS joints** in **14-19 K** range**;** verified **electro-magnetic compatibility** among the various circuits.

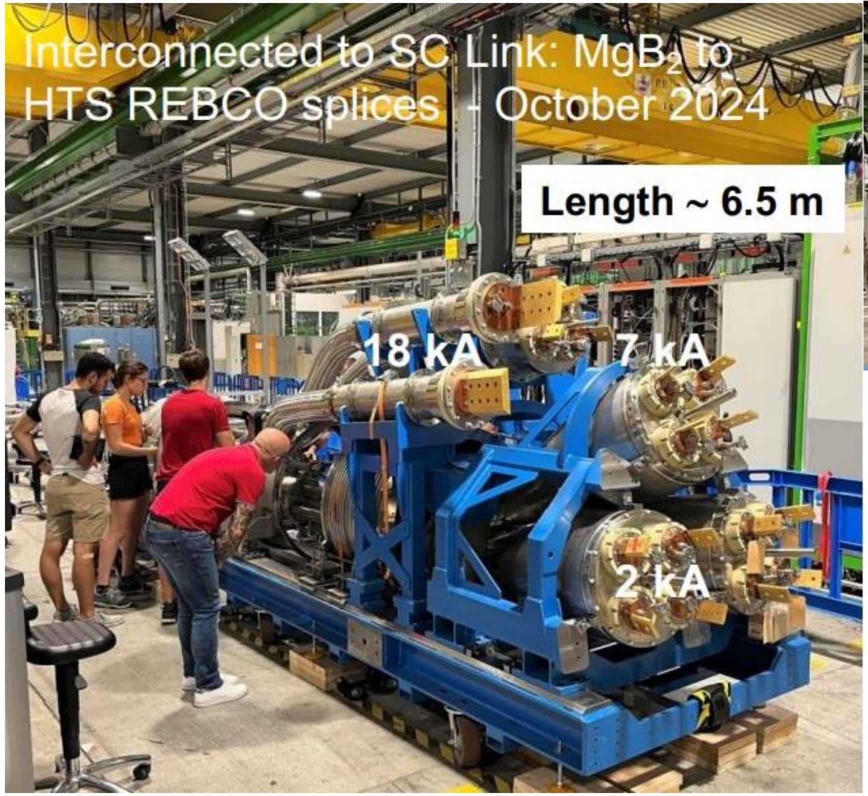

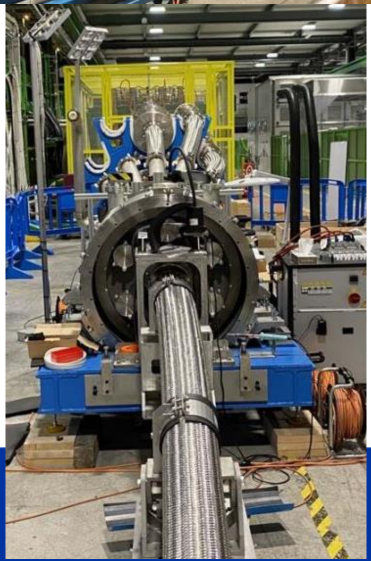

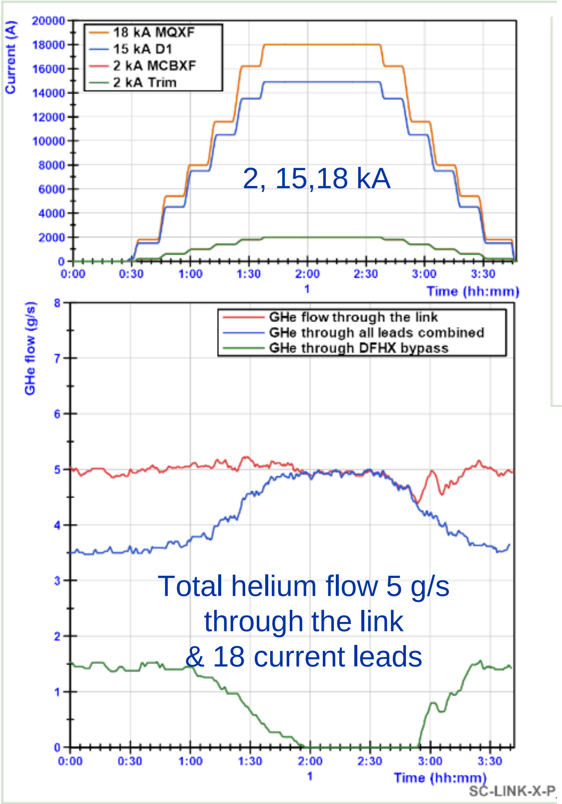

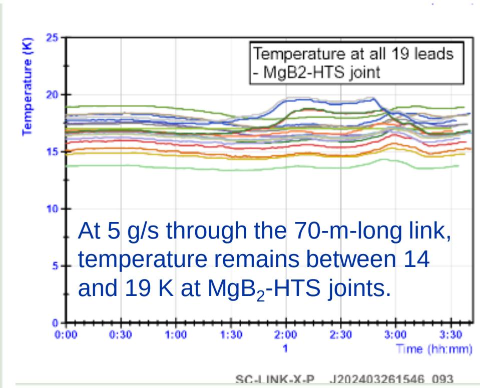

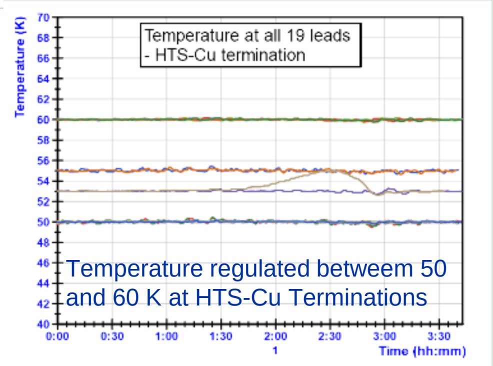

Courtesy of G. Willering
(CERN TE-MSC)

HL-LHC Nb_3Sn Magnets

- HL-LHC initially envisioned relying on **two types of Nb_3Sn magnets**

(1) pairs of **5.3-m-long, 60-mm-twin-aperture dipole magnets** (referred to as “11 T”) for installation in two dispersion suppressor areas, to replace existing 15-m-long LHC dipole magnets and make room for **additional collimators;**

(2) sets of large, **150-mm-single-aperture quadrupole magnets** (referred to as MQXF) for installation in the **interaction regions** of the 2 high-luminosity LHC experiments (ATLAS and CMS).

- The four (plus 2 spares) **11 T dipole magnets** are based on a **design initially developed at Fermilab** circa 2010 and were supposed to be produced **at CERN;**

- The **quadrupole magnets** are based on a **design developed within the framework of the US LHC Accelerator Research Program (LARP),** initiated in 2003, and come in 2 lengths

– 16 (plus 4 spares) **4.2-m-long MQXFA magnets** under production by the **U.S. HL-LHC Accelerator Upgrade Project (AUP;** started in 2018);

– 8 (plus 2 spares) **7.2-m-long MQXFB magnets** under production **at CERN.**

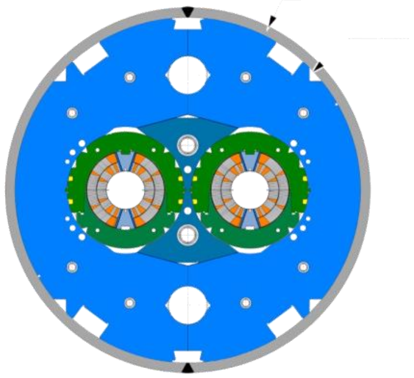

11 T Dipole Magnet X-Section
Courtesy of F. Savary
(CERN TE-MSC)

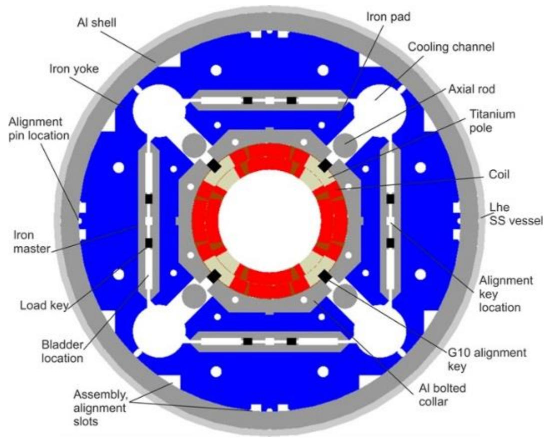

MQXF Quadrupole Magnet X-Section
Courtesy of E. Todesco
(CERN TE-MSC)

Short HL-LHC Nb_3Sn Model Magnets

- HL-LHC has two levels of **performance requirements** for its magnets
  - **nominal level,** corresponding to **7.0 TeV** operation;
  - **ultimate level,** corresponding to 7.5 TeV operation.
- Both **HL-LHC Nb_3Sn dipole** and **quadrupole magnet programs** have produced **successful short model magnets** that demonstrate **feasibility,** achieving nominal and even ultimate currents (and beyond) with a limited number of quenches at 1.9 K.
- For 11 T, nominal current is **11.85 kA** and bore/peak fields are **11.22/11.77 T;** ultimate current is **12.84 kA** and bore/peak field are **12.14/12.74 T (at 1.9 K).**
- For **MQXF,** nominal current is **16.23 kA** and gradient/peak fields are **132.6 T/m/11.4 T;** ultimate current is **17.5 kA** and gradient/peak field are **141.4 T/m/12.1 T (at 1.9 K).**

Initial Training of short 11 T dipole model magnets

Courtesy of G. Willering (CERN TE-MSC)

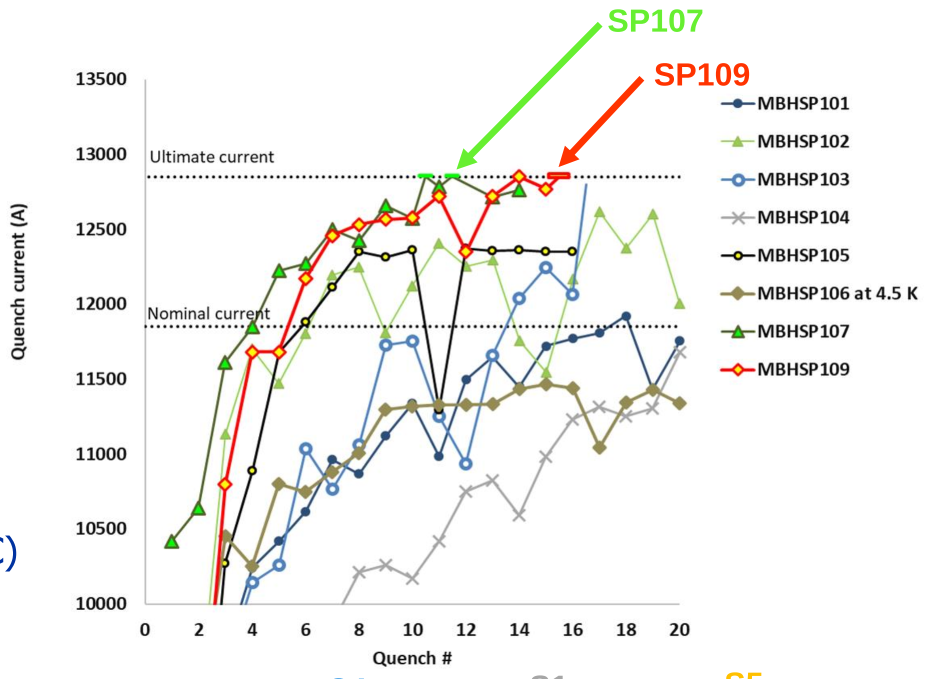

Initial Training of short MQXFS quadrupole model magnets

Courtesy of F. Mangiarotti (CERN TE-MSC)

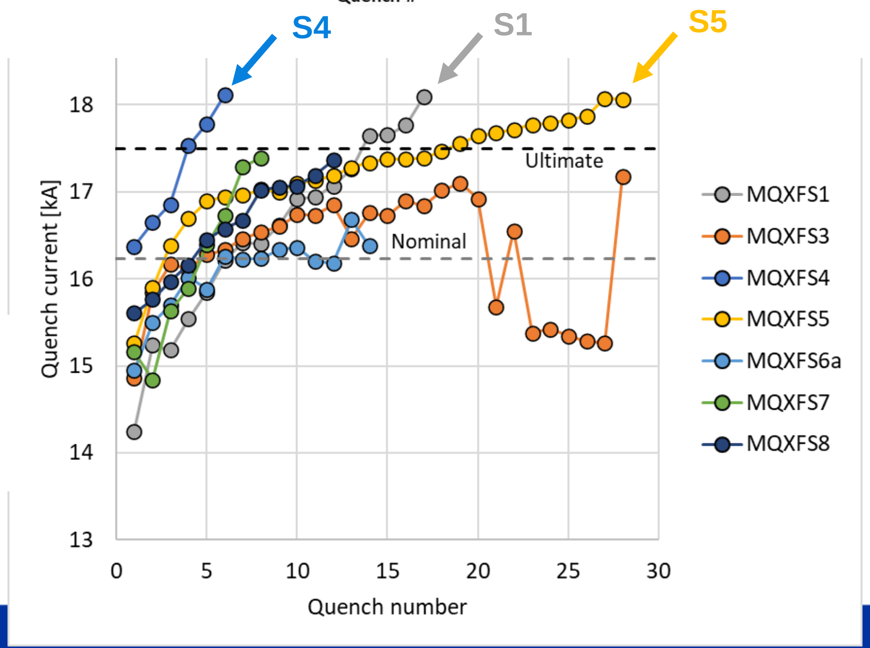

Long (> 5 m) HL-LHC Nb_3Sn Prototype Magnets @CERN

- Problems arose in 2020/2021 with the power testing of **full-length (> 5 m) HL-LHC Nb_3Sn magnets** at CERN.
- First **11 T dipole** series magnet (S1) reached nominal current after 2 training quenches and exhibited no re-training after warm-up/cooldown cycle, but subsequent series magnets (S2-S4) exhibited **performance degradation,** either upon first cooldown (S3), or after two or more cooldowns (S2 and S4).
- First and second **MQXFB quadrupole** prototype magnets (P1 and P2) exhibited **performance limitation below nominal current.**
- These results triggered the decision in **Q4 2020** **not to install 11 T dipole magnets** in the LHC machine and to put **MQXFB production activities on hold** in **Q2 2021.**

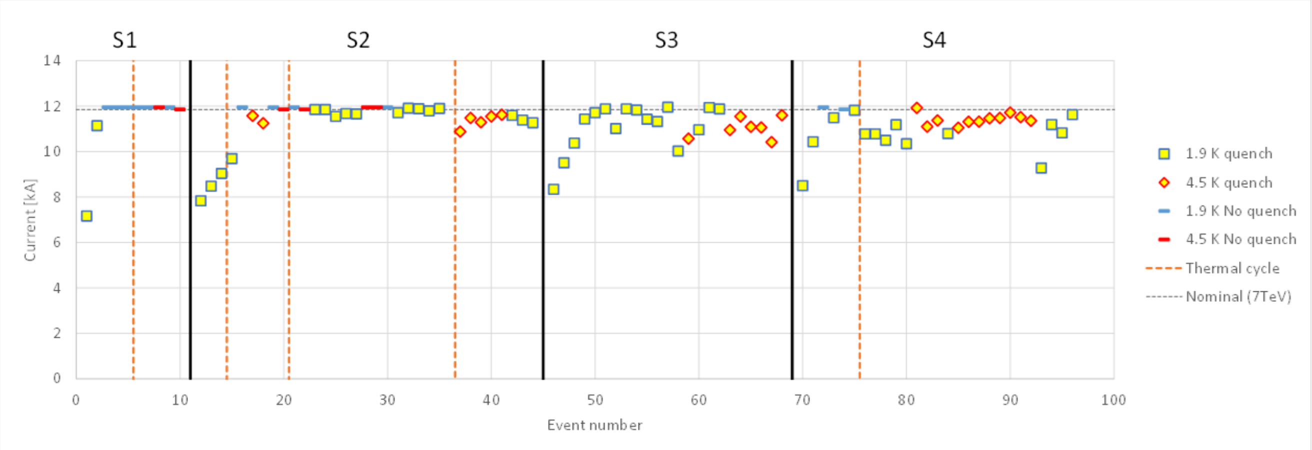

Quench Performance of 5.3-m-long, 60-mm-twin-aperture 11 T Dipole Series Magnets

Courtesy of G. Willering
(CERN TE-MSC)

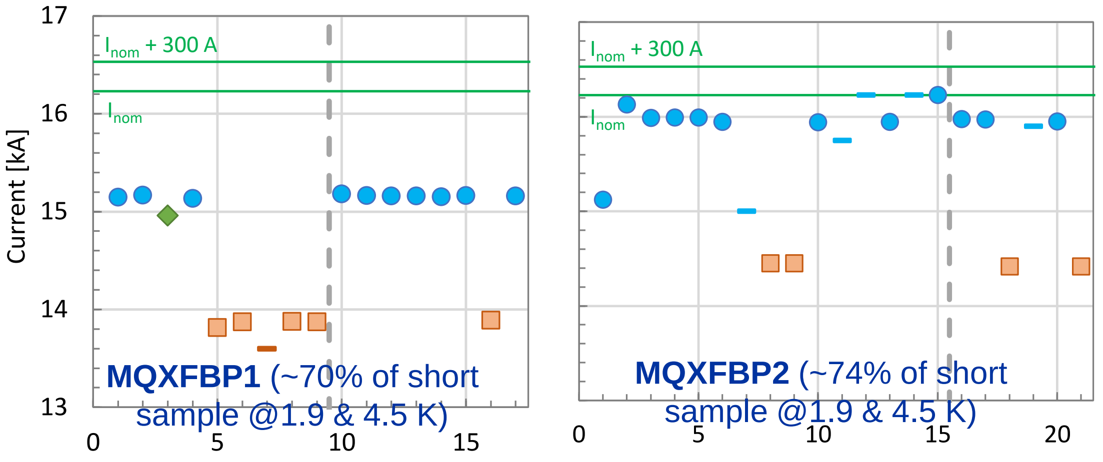

Courtesy of F. Mangiarotti
(CERN TE-MSC)

Quench Performance of 7.2-m-long, 150-mm-single-aperture MQXFB Quadrupole Prototypes Magnets

HL-LHC Nb_3Sn Magnets vs. ITER Nb_3Sn CICCs

- The test results of the **long HL-LHC Nb_3Sn magnets** at CERN generated **concerns and questions** about the **viability of Nb_3Sn technology,** similar to those that were raised over a decade earlier at ITER with the **SULTAN test results of the early TF and CS conductor samples.**

- As in the case of ITER, the problem compounded surprisingly similar **technical, human and management factors.**

- **The ITER experience and methodology** were very useful to **identify corrective actions** and develop **recovery plans** (see next slides).

Performance Degradation of early ITER CS conductor performance qualification samples

Courtesy of Y. Nunoya & Y. Takahashi (QST)

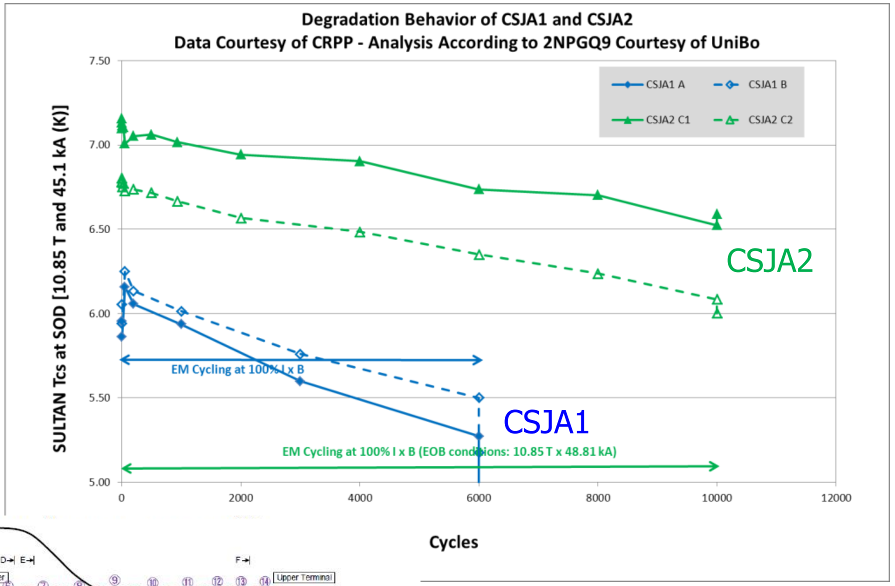

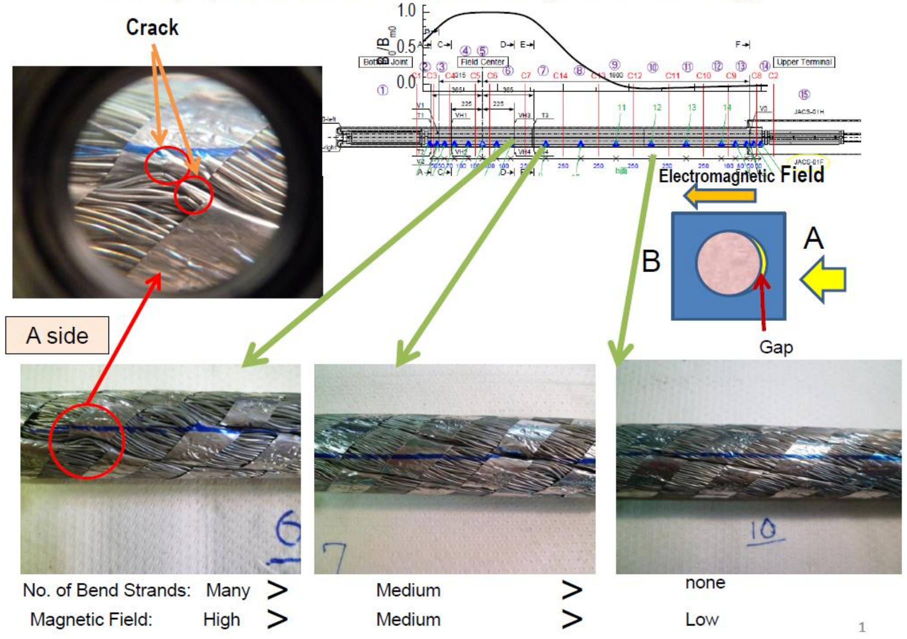

Non-Compressive Side

EM Force

Improved Diagnostics and Post-Mortem Examinations on Nb_3Sn Magnets

Symptoms

Improved Diagnostics

Post-Mortem Examinations

Symptoms (1/2): Performance Limitation

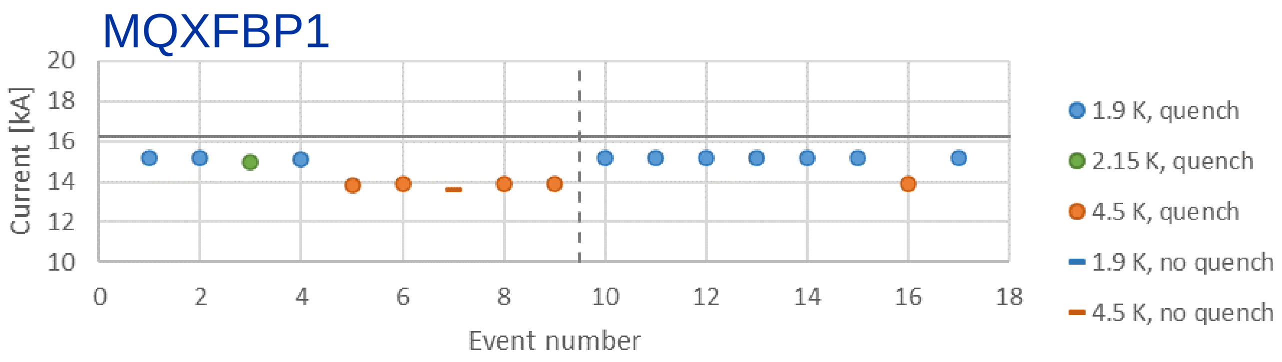

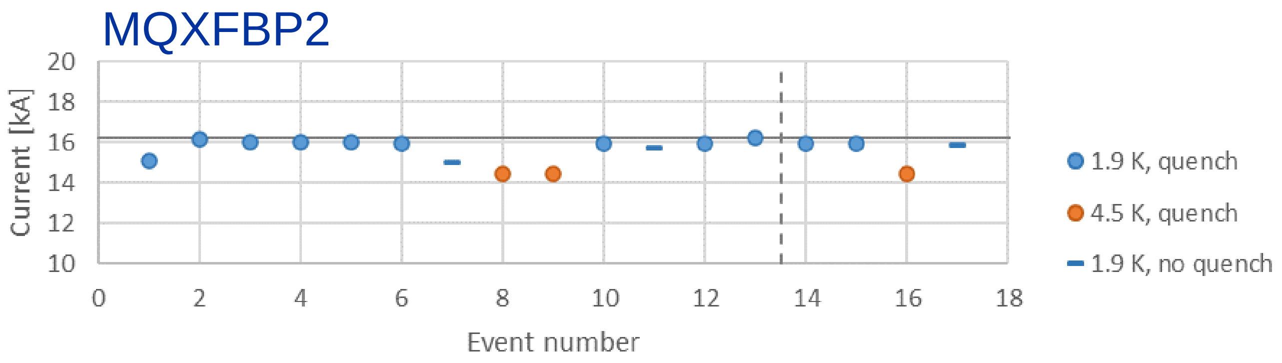

Quench Performance of MQXFBP1&2 (7.2-m-long, 150-single-aperture, HL-LHC quadrupole magnet prototypes)

Courtesy of F. Mangiarotti

(CERN/TE-MSC)

- Magnet reaches a **performance plateau** after first cooldown **below target current.**
- **Reproducible** quench location (mostly towards magnet **mechanical center** for MQXFB quadrupole magnets).
- **Proper scaling between 1.9 K and 4.5 K** and **regular ramp rate behaviour.**
- Reproducible behaviour **after WUCD cycle.**

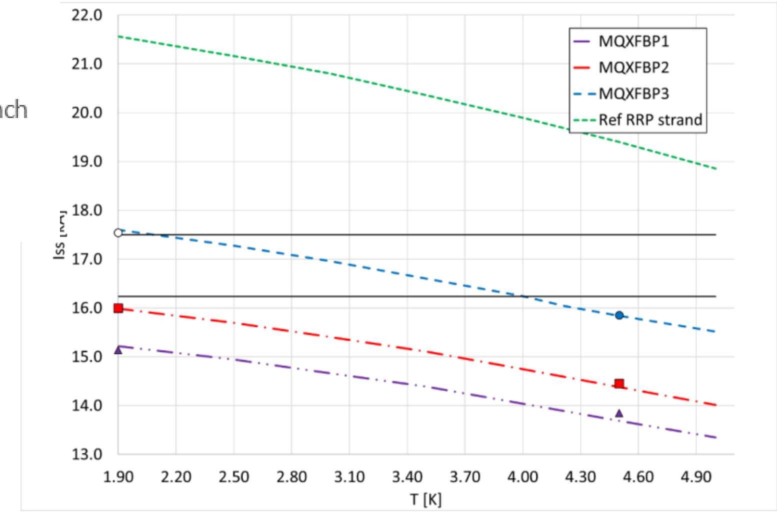

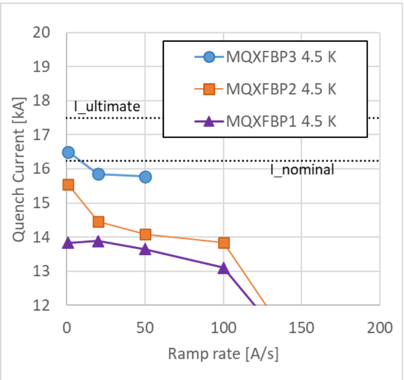

Symptoms (2/2): Performance Degradation

- Magnet exhibits a **performance degradation** after a **sequence of EM and WUCD cycles.**
- Quench location mostly in **coil heads** (for 11 T dipole magnets) but affected by **type of current ramp.**
- Performance **does not scale with temperature** and can exhibit **irregular ramp rate behavior**.
- Impacted by **WUCD.**

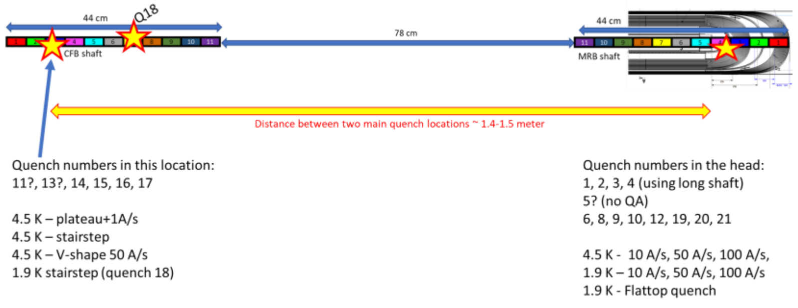

Quench start localization in S4 series magnet

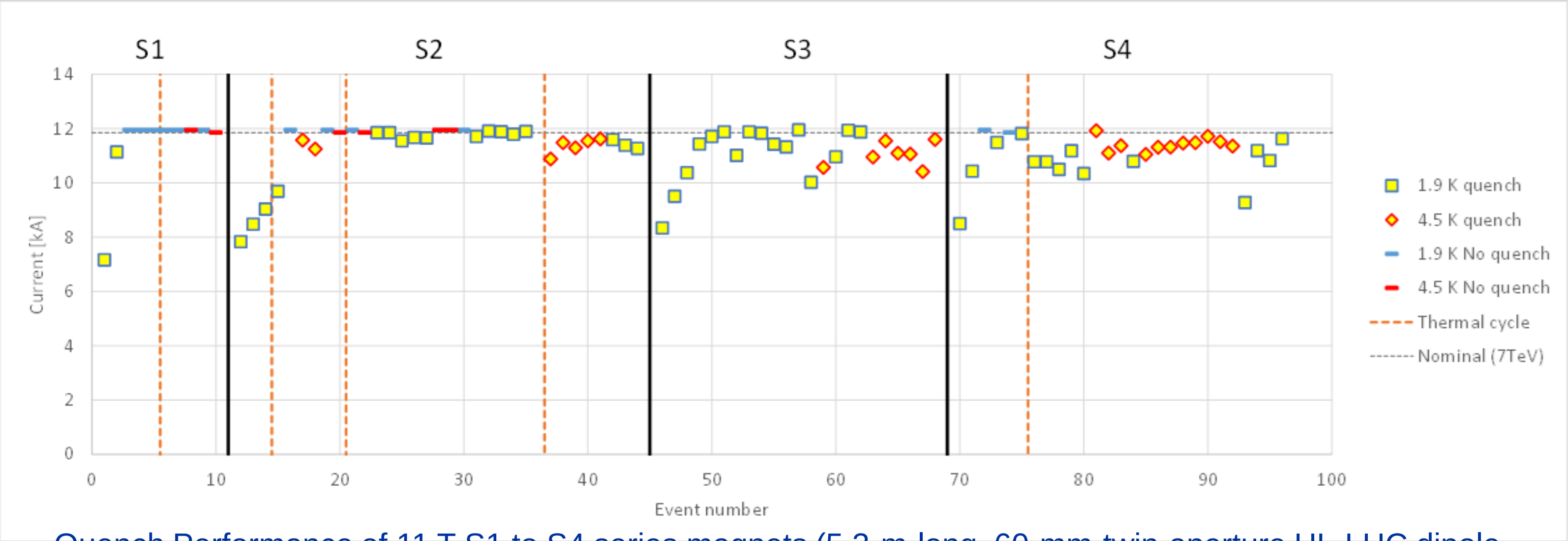

Quench Performance of 11 T S1 to S4 series magnets (5.3-m-long, 60-mm-twin-aperture HL-LHC dipole magnets)

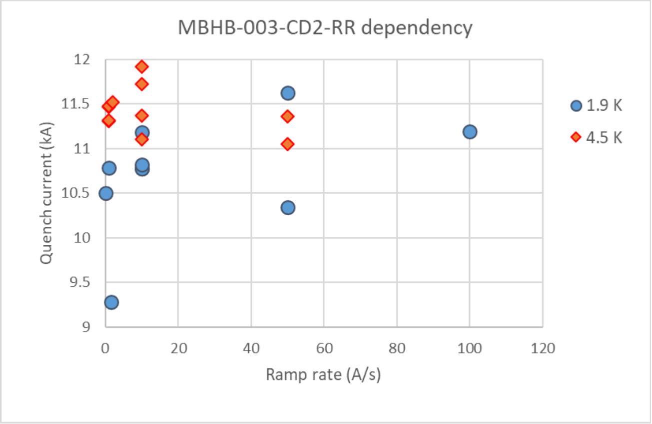

Ramp-rate sensitivity of S4 series magnet

Courtesy of G. Willering
(CERN/TE-MSC)

Improved Diagnostics (1/3): *V-I* Measurements

- **Sensitive voltage measurements** can be carried during magnet testing, enabling **early detection of resistive transitions** and **monitoring of their evolutions** after electromagnetic and thermal cycling.
- Technique was successfully developed in later part of 11 T short models and series magnets **(circa 2018);** it can be applied to **full coil voltages.**

Courtesy of G. Willering
(CERN/TE-MSC)

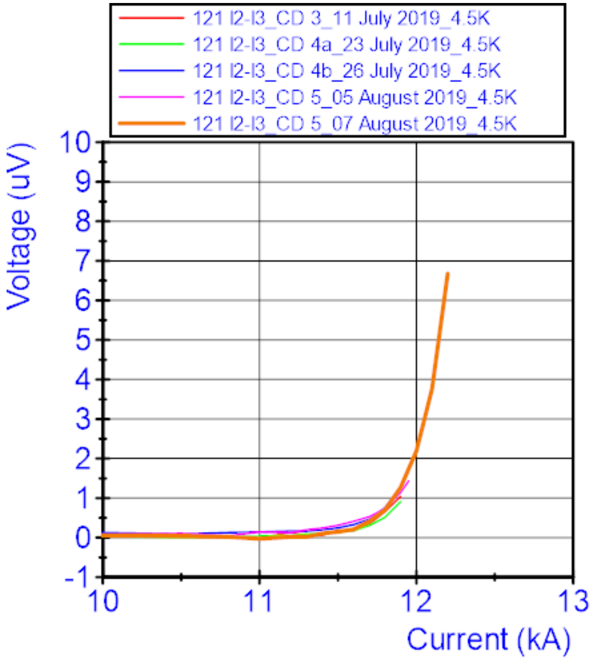

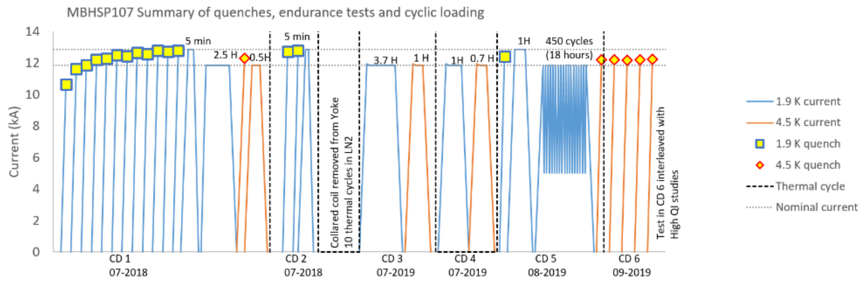

Stable Behavior

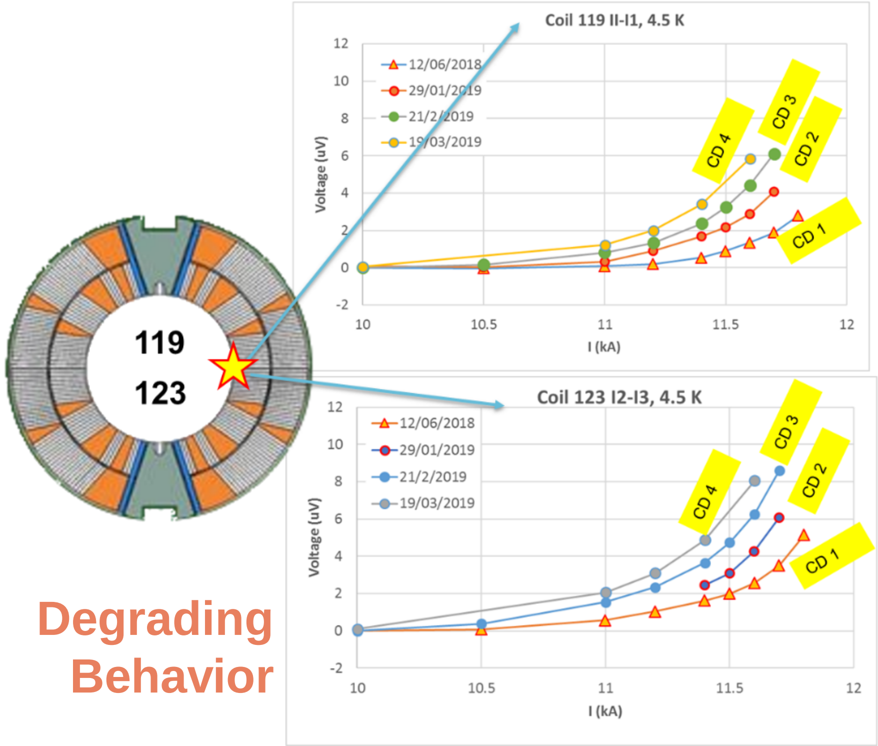

Degrading Behavior

Example of stable behavior: short, 11 T Dipole Magnet Model SP107

Example of degrading behavior: short, 11 T Dipole Magnet Model SP109

Improved Diagnostics (2/3): Trim Powering

- In case of a magnet whose quench performance is **limited by one coil,** the trim powering procedure enables **injection of additional current in the other coils** to assess their behavior (concept initially proposed by A. Milanese, CERN/TE-MSC).
- It is now successfully applied for the power tests of **short and long MQXFB quadrupole magnets.**

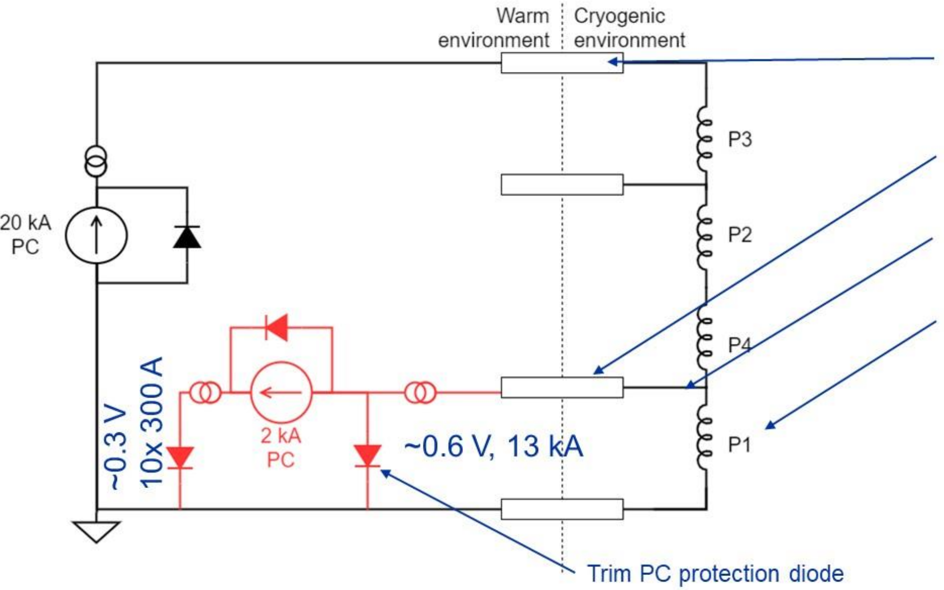

Electrical Circuit for Trim Power Test

Courtesy of F. Mangiarotti
(CERN/TE-MSC)

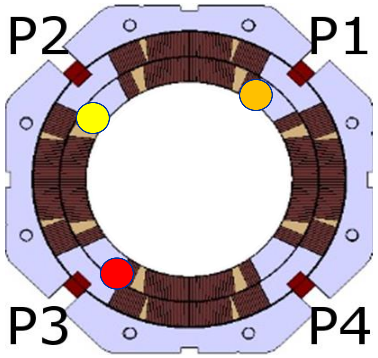

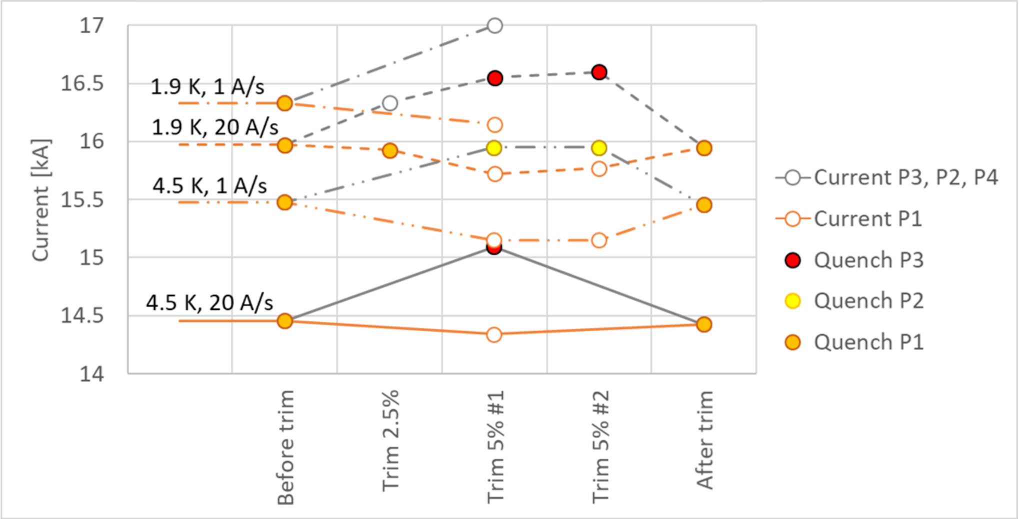

Trim powering test results for 7.2-m-long MQXFBP2 at CERN, showing that 3 out of 4 coils were performance-limited with similar phenomenology.

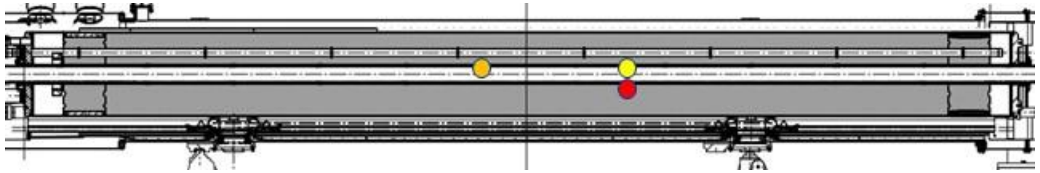

Improved Diagnostics (3/3): 3D Quench Antenna – 1/2

- CERN has implemented since **Summer 2022** a **quench antenna** configuration relying on **coils sensitive to multipole components** (*e.g.*, B_3, A_3, B_4, A_4 for a quadrupole magnet) following a concept initially proposed by **T. Ogitsu** at **SSC Laboratory,** circa **1992.**
- The system, based on flexible **Printed Circuit Boards (PCBs),** enables accurate **azimuthal quench start localization;** it is less accurate in the **longitudinal direction,** where it requires **segmentation.**
- The system was upgraded recently to integrate, on top of the **4** baseline, **straight PCBs,** another set of **2 helically twisted PCBs** to enable higher accuracy on the **longitudinal quench start localization** (based on phase shift).

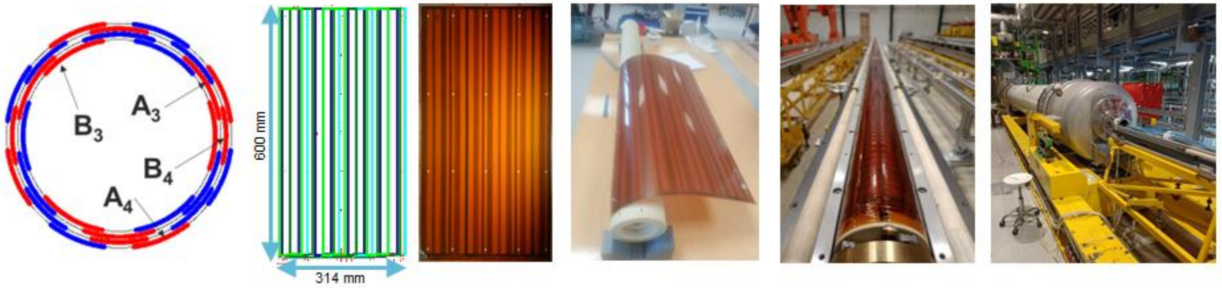

Design, assembly, and implementation of new quench antenna system

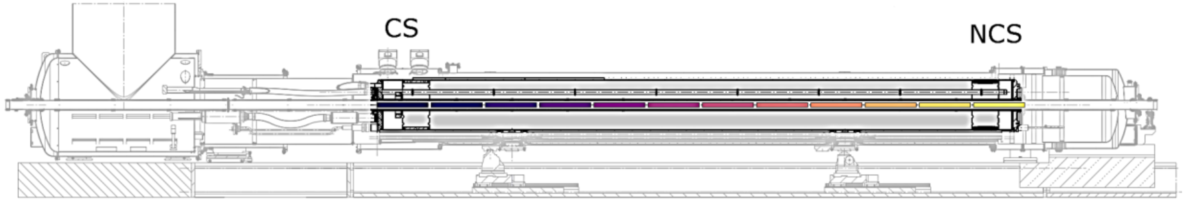

Several segments needed to cover the magnet length

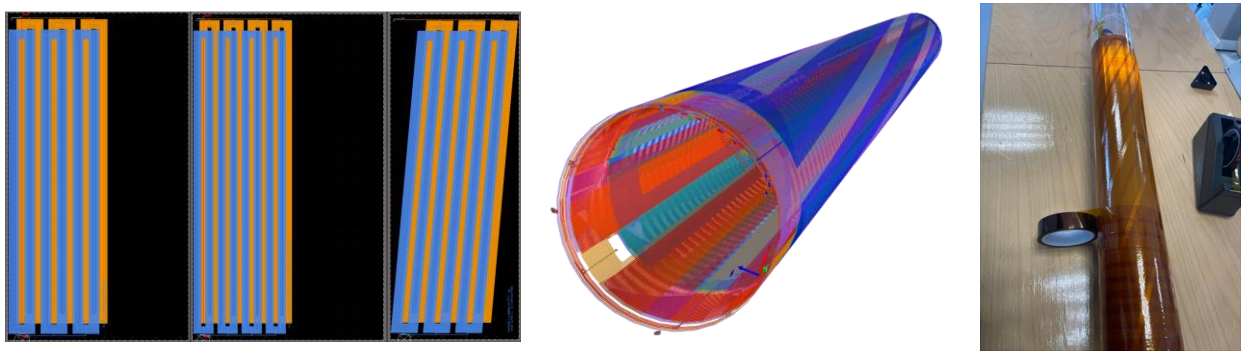

B_3, A_3 B_4, A_4 B_3, A_3 twisted

Upgraded system with additional twisted coils

Courtesy of L. Fiscarelli and P. Rogacki (CERN/TE-MSC)

Improved Diagnostics (3/3): 3D Quench Antenna – 2/2

- The **upgraded system** has been successfully tried on 2 MQXFB quadrupole magnets **(MQXFBP2** and **MQXFBP3)** and one D1 dipole magnet **(MBSFP1).**
- The new system also enables comprehensive analyses of **flux jumps while ramping.**

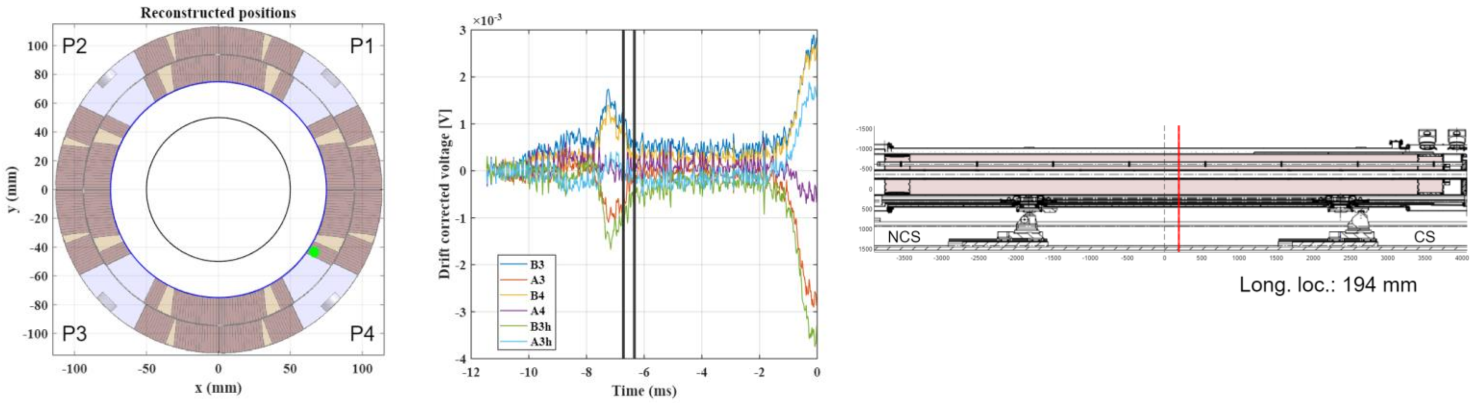

Localization of 4.5 K limiting quenches in MQXFBP3 (retested in final Q2 configuration)

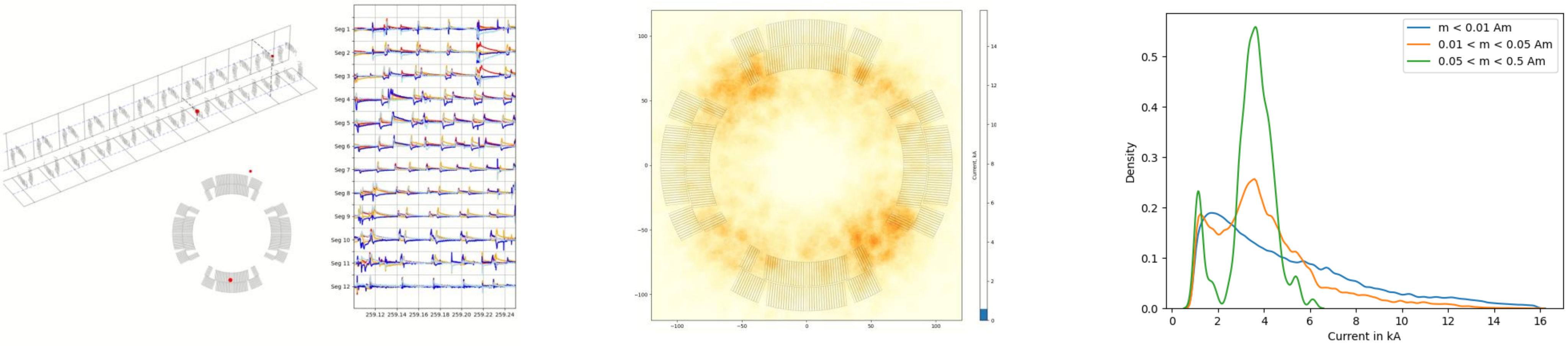

Observation of flux jumps while ramping (can be analyzed in terms of position, amplitude, orientation, and propagation

Courtesy of L. Fiscarelli and P. Rogacki
(CERN/TE-MSC)

Post-Mortem Examinations (1/4): Overview

- Starting from June 2019, the team of S. Sgobba in CERN/EN-MME has developed a methodology to carry **out post-mortem examinations** of **sections of HL-LHC dipole and quadrupole magnet coils** that exhibited performance limitation and/or degradation.
- Examination starts from **mesoscale observation** of a **whole coil volume** (typically, the volumes where the quench origins have been localized).
- **Different techniques** are gradually applied to get more detailed insights into internal events, geometrical distortions, and possible flaws, down to the **microscopic scale.**

Courtesy of I. Aviles Santillana (CERN/EN-MME)

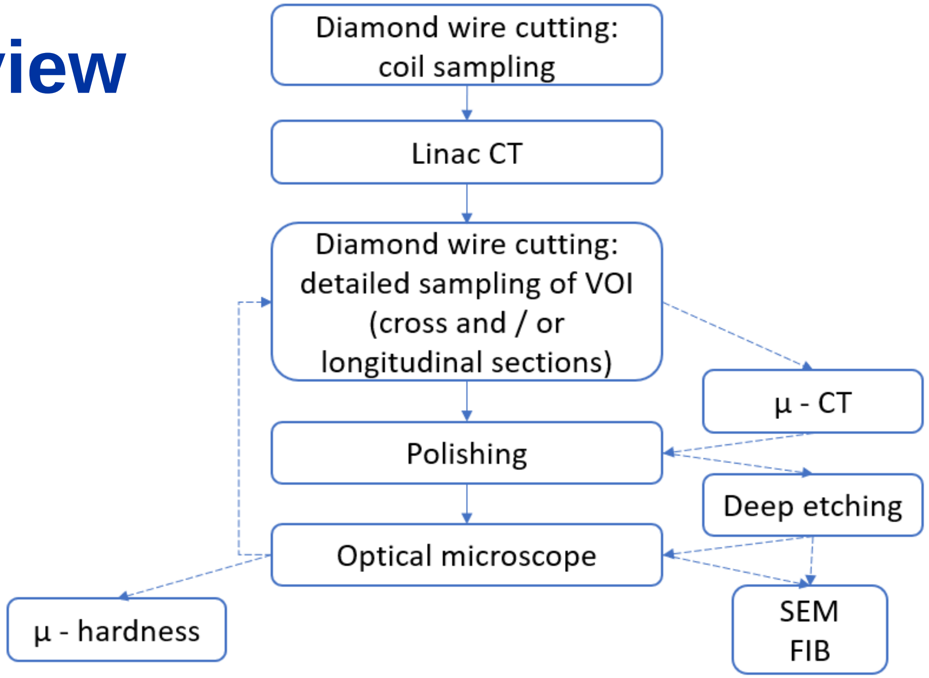

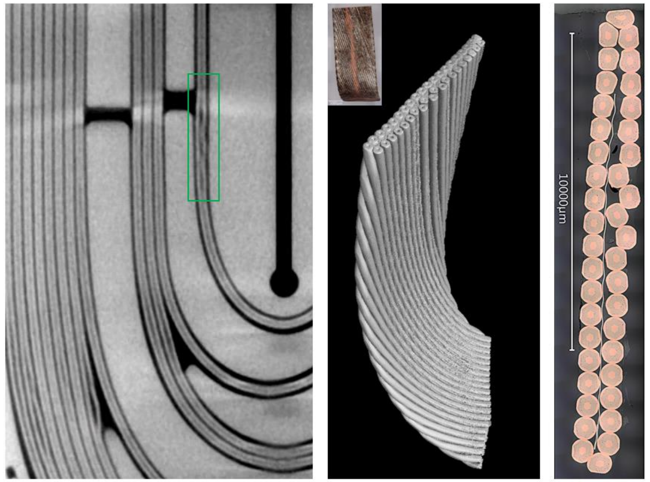

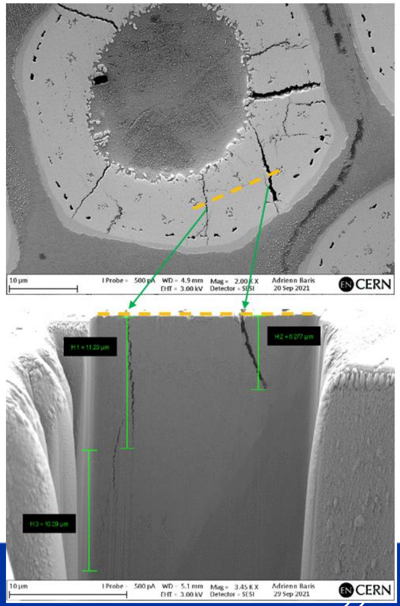

Post-Mortem Examinations (2/4): High-Energy X-Ray Tomography

Courtesy of S. Sgobba
(CERN/EN-MME)

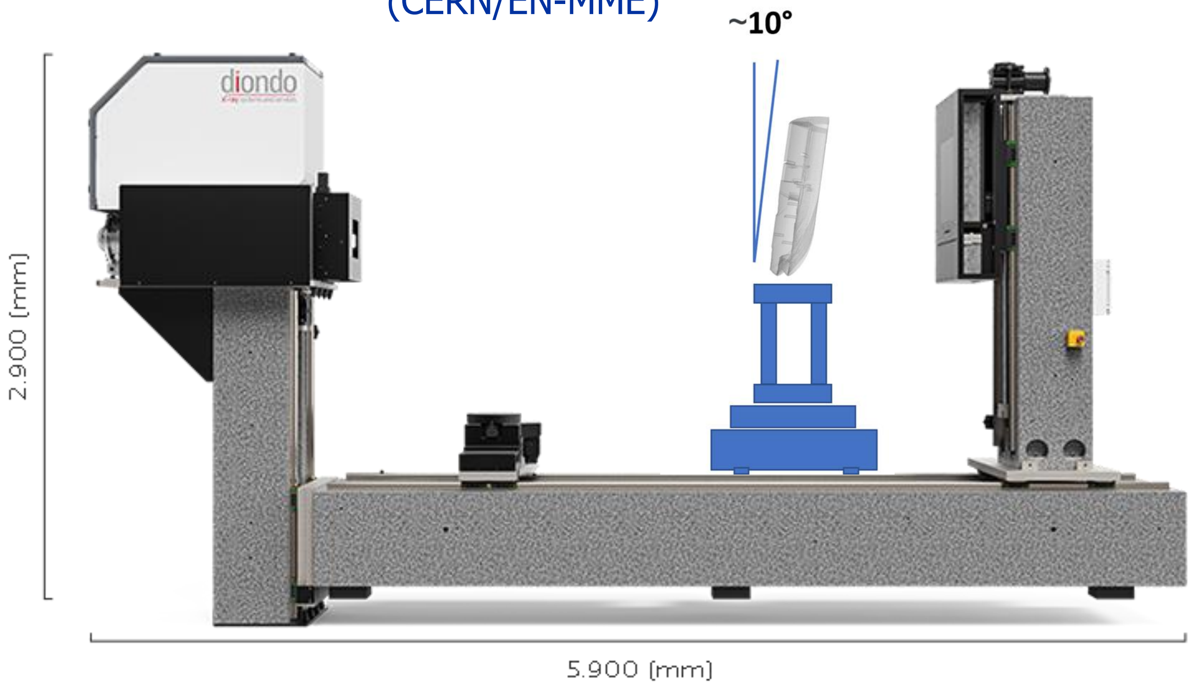

- First step is **high-energy X-ray computed tomography,** which has proven to be an efficient tool for **inspecting 20-30 cm coil samples** (including whole coil ends)**.**
- The system relies on a **6 MeV LINAC;** it has a spot size of 2 mm and a **resolution of ~120 μm.**

Examples of analyses by X-ray tomography of the end of a 5.3-m-long, 11 T dipole magnet coil (GE2) where most limiting quenches had been localized

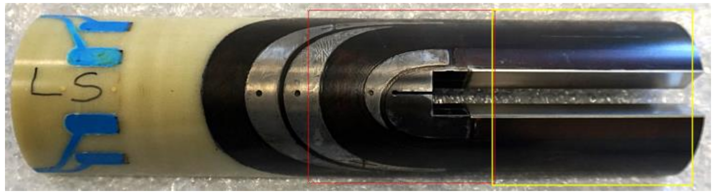

Event 1 – first end cable in inner layer
Misaligned strands
(pop-in / pop-out)

Event 2 – vicinity of fourth spacer in inner layer
Bulged cable

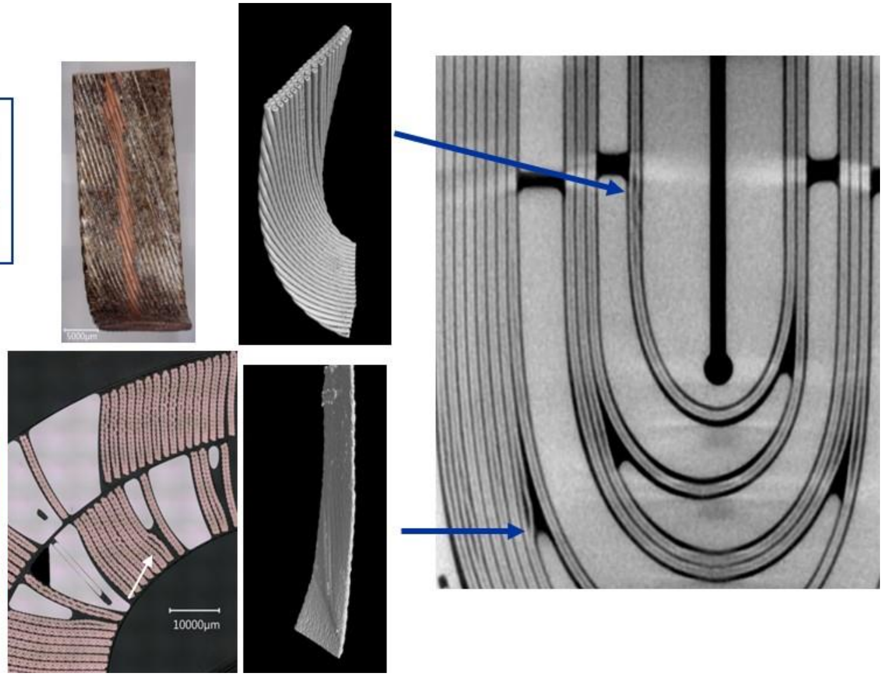

Post-Mortem Examinations (3/4): Metallographic Analyses

- Second step is to carry out **metallographic analyses** in the zones of interest identified by computed tomography.
- Direct visualization of **internal defects: strand displacements,** and **cracks in Nb_3Sn sub-elements** and in **epoxy resin.**

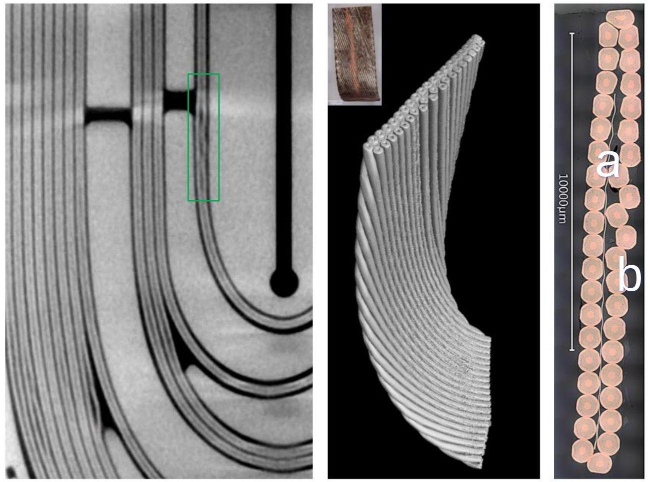

Analyses of a zone of interest in of the end of 5.3-m-long, 11 T dipole magnet coil GE2 (see previous slide)

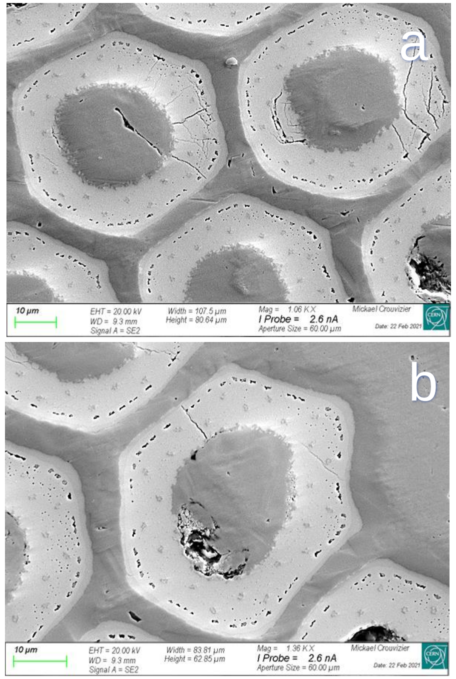

Courtesy of M. Crouvizier (CERN/EN-MME)

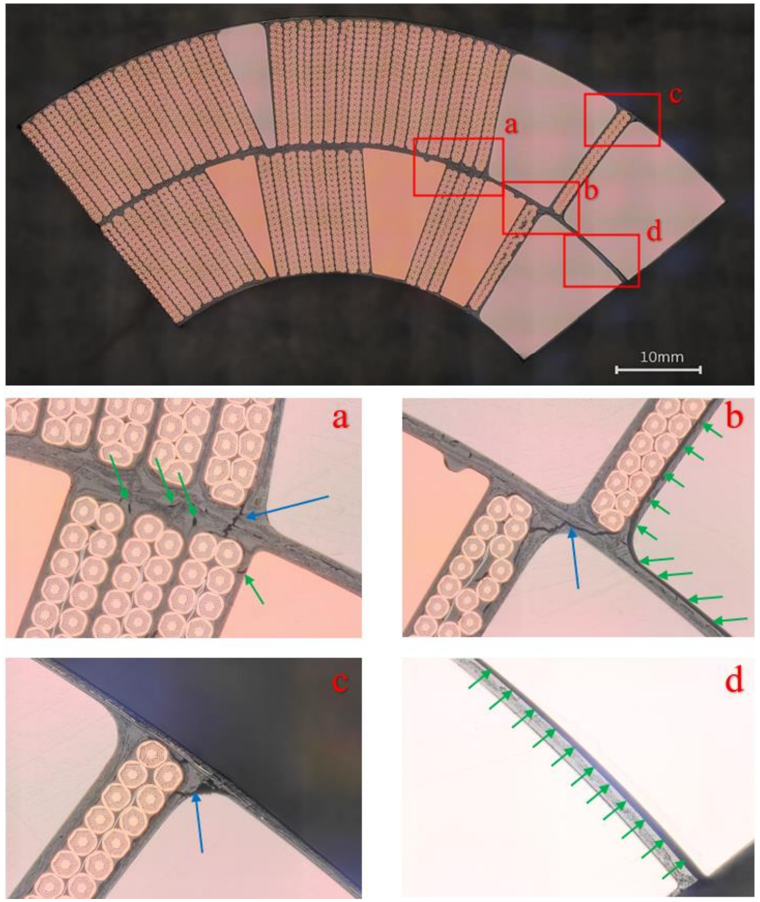

Analyses of 5.3-m-lonh, 11 T dipole magnet coil GE13 (used in series magnet S2): (a) **shrinkage cavities** (green arrows) and **metal-to-metal crack** across the coil interlayer (blue arrow); (b) **metal-to-metal crack** (blue arrow) and **large decohesion** (green arrows); (c) **conductor–to–pole crack** (blue arrow); (d) **large decohesion between resin and pole piece** (green arrows)

Post-Mortem Examinations (4/4): Analyses After Deep Cu Etching

- Third step is to apply **deep Cu etching** and **microscopy** to assess the extent of **Nb_3Sn sub-elements damages.**
- In limiting, long MQXFB coils, the area of **quench start localization** (towards the magnet center) appears **correlated with sub-element damages** observed in **one specific cable strand** (out of 2000), at the **top of the inner-layer pole turn,** underneath a corner of the outer layer Ti-pole.

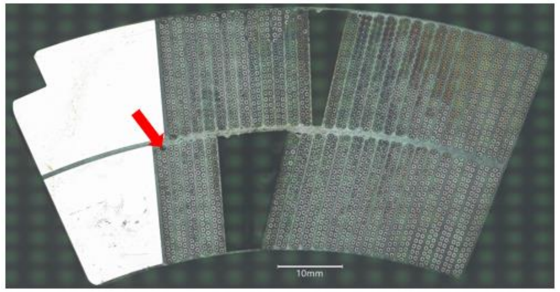

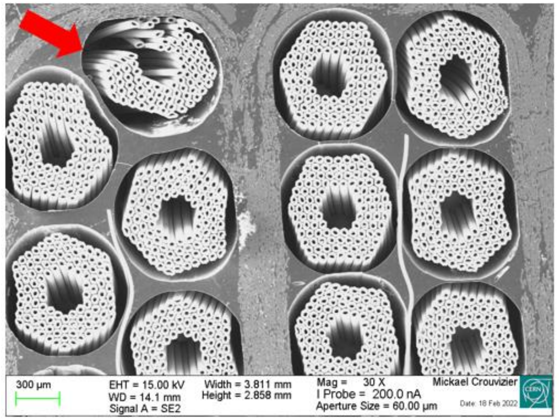

- The **grain morphology** at the fracture surface of the ruptured sub-elements seems to indicate that the damage occurred **after completion of the high-temperature plateau** of the heat treatment.

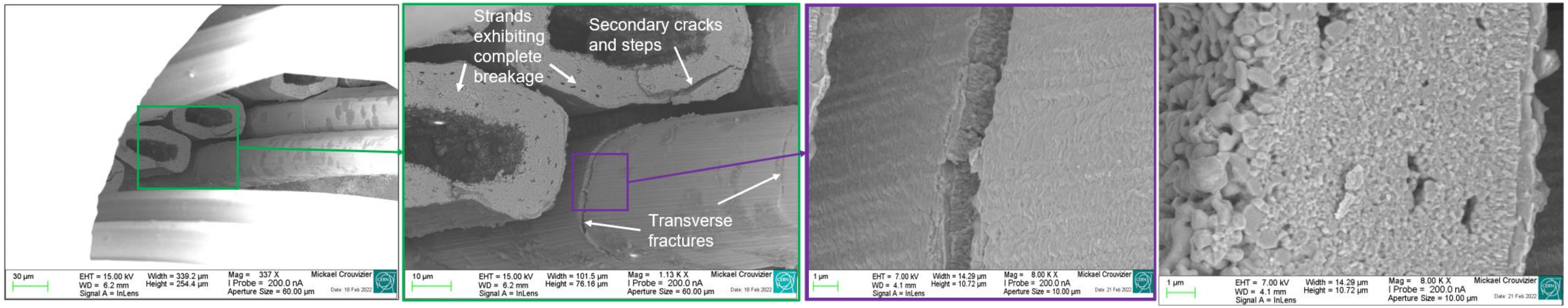

Fracture surfaces of Nb_3Sn sub-elements observed in damaged strand (at top of inner-layer pole turn) in MQXFBP1 quadrupole magnet coil CR108 where limiting quenches were localized

Courtesy of M. Crouvizier
(CERN/EN-MME)

Complementary Post-Mortem Examinations (1/3)

Courtesy of M. Crouvizier and A. Moros (CERN/EN-MME), **and S. Izquierdo Bermudes** (CERN/TE-MSC)

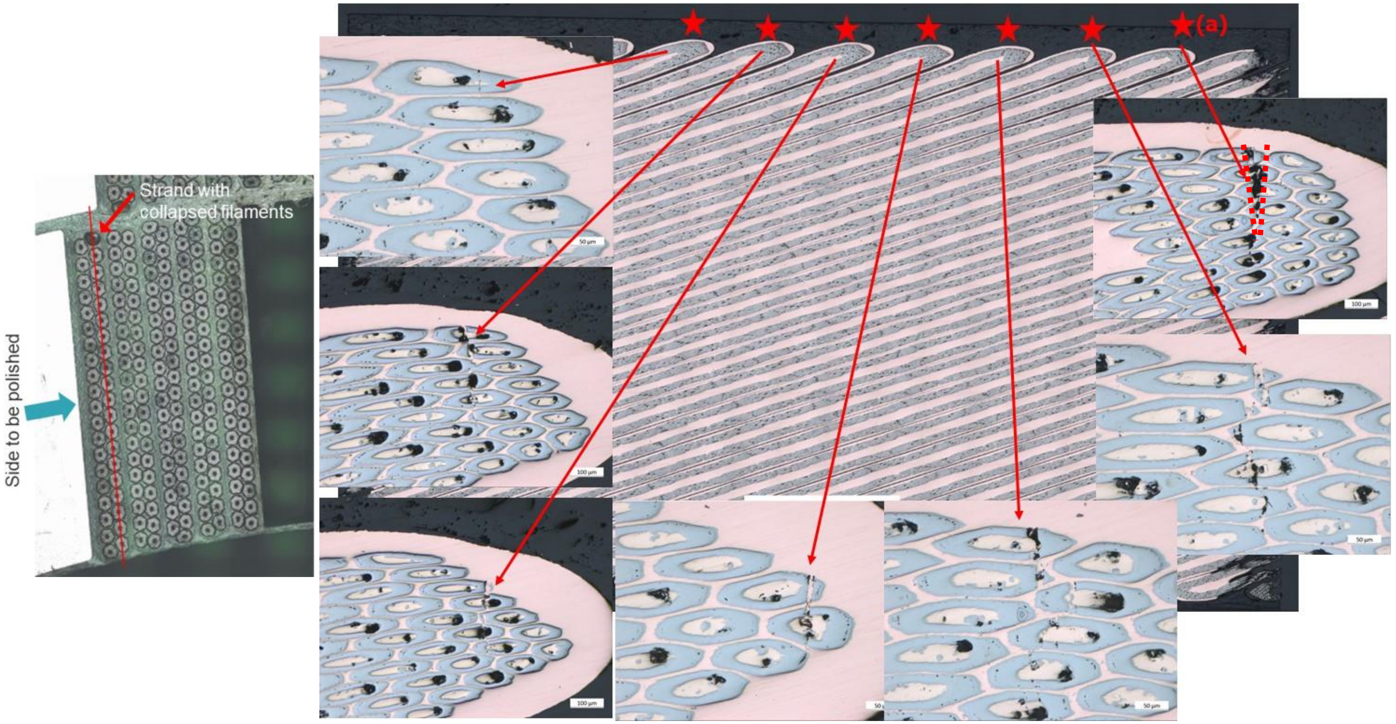

Metallographic analyses of a longitudinal cut of row of strands of inner pole turn cable where damaged strand has been observed in transvers cut; neighboring strands are also damaged.

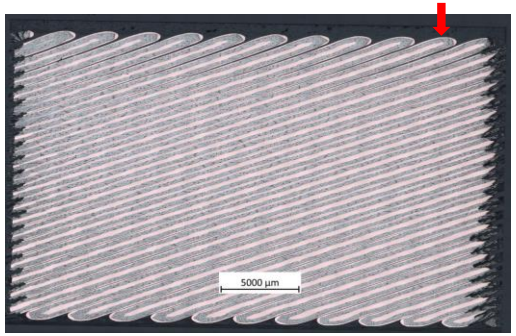

Examples of V-shape fracture surface analyses

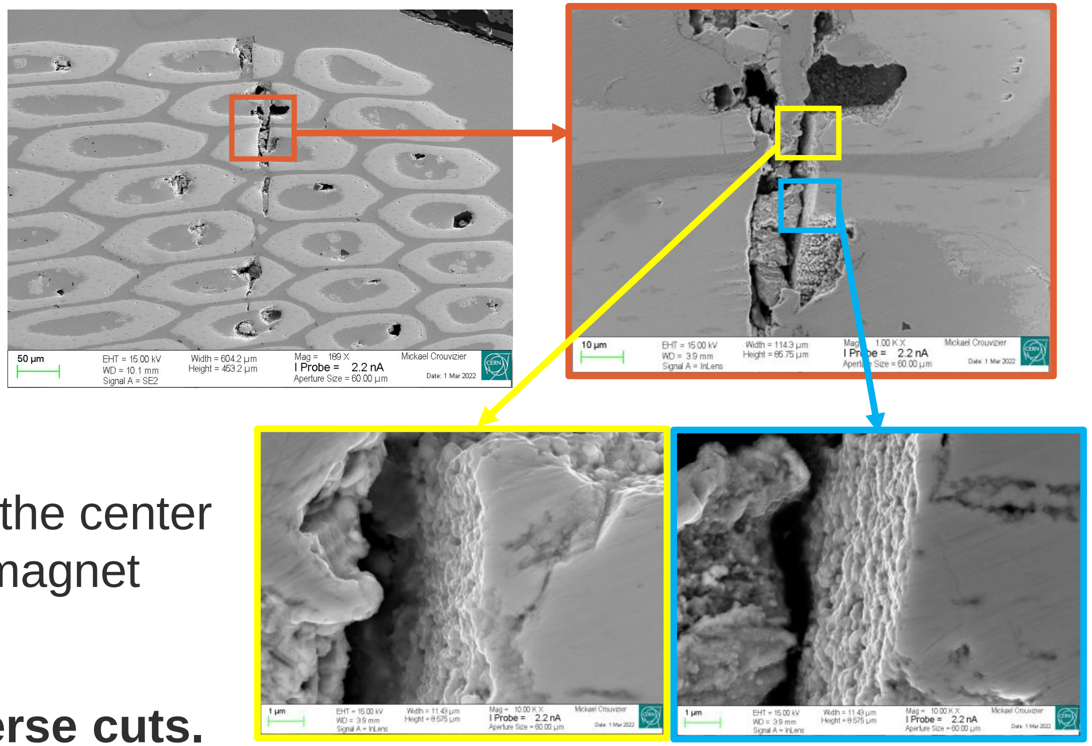

- Metallographic analyses carried out on a **longitudinal cut** near the center of the layer-jump side of the **limiting coil** of HL-LHC quadrupole magnet prototype MQXFBP1 (CR108) show a typical ***V*-shape fracture.**

- Analysis of **fracture surfaces** confirms observations on **transverse cuts.**

Complementary Post-Mortem Examinations (2/3)

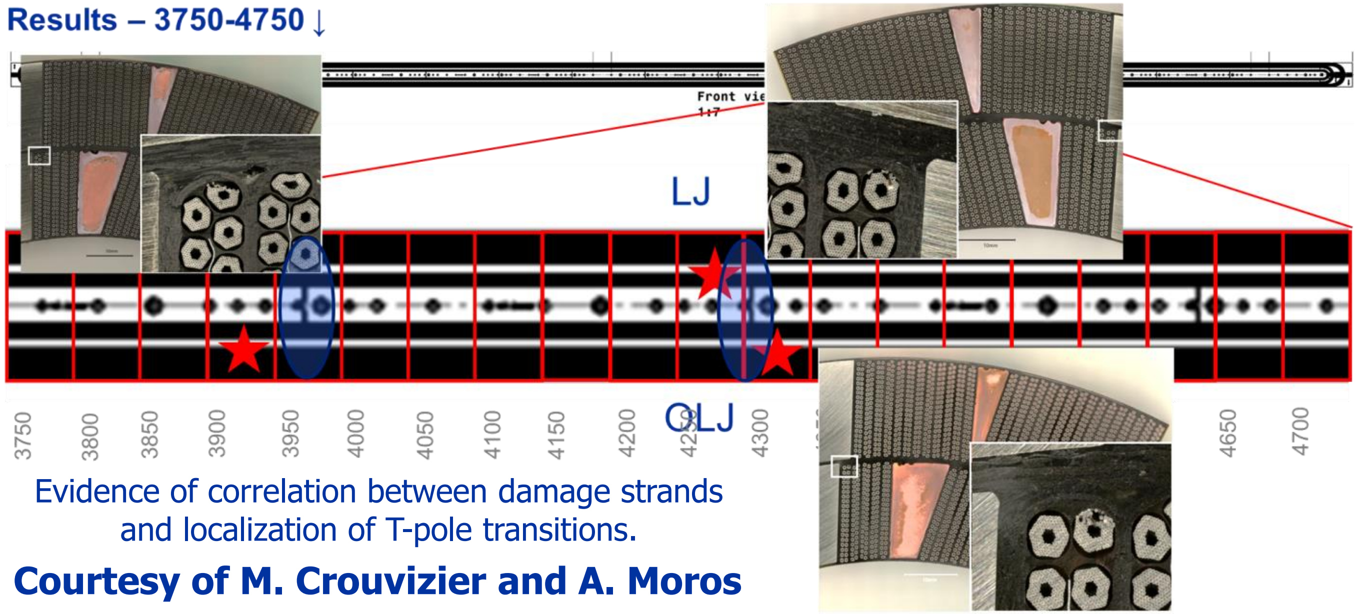

Evidence of correlation between damage strands and localization of T-pole transitions.

Courtesy of M. Crouvizier and A. Moros (CERN/EN-MME), **and S. Izquierdo Bermudes** (CERN/TE-MSC)

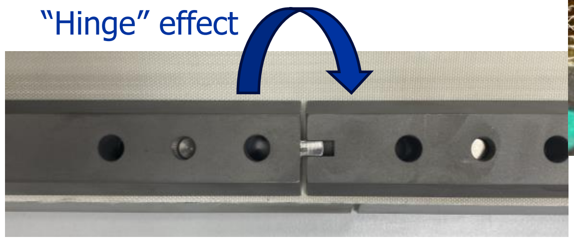

Interpole gap is set up at time of winding (0.9 to 1.5 mm depending on coils)

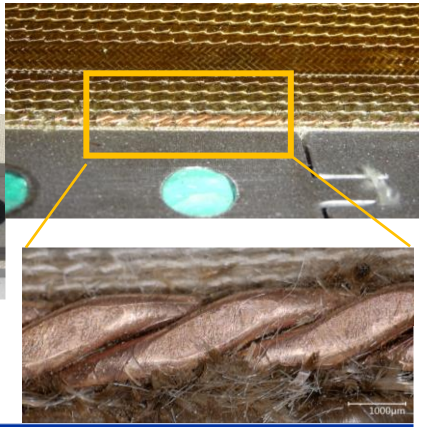

Evidence of inner pole turn protrusion and insulation damage at the location of Ti-pole transition.

Courtesy of N. Lusa and A. Milanese (CERN/TE-MSC)

- From the extensive analyses carried out on the **limiting coil** of HL-LHC quadrupole magnet prototype MQXFBP1 (CR108), the **longitudinal positions where damages are observed** on the strand at the top of the inner-layer pole turn are always in the vicinity of a **Ti-pole transition.**
- The origin of the damage is likely to be a **"hinge" effect** at the Ti-pole transitions that causes a **local displacement/ deformation of the inner layer pole turn** when opening/closing heat-treatment and/or vacuum pressure impregnation molds.

Complementary Post-Mortem Examinations (3/3)

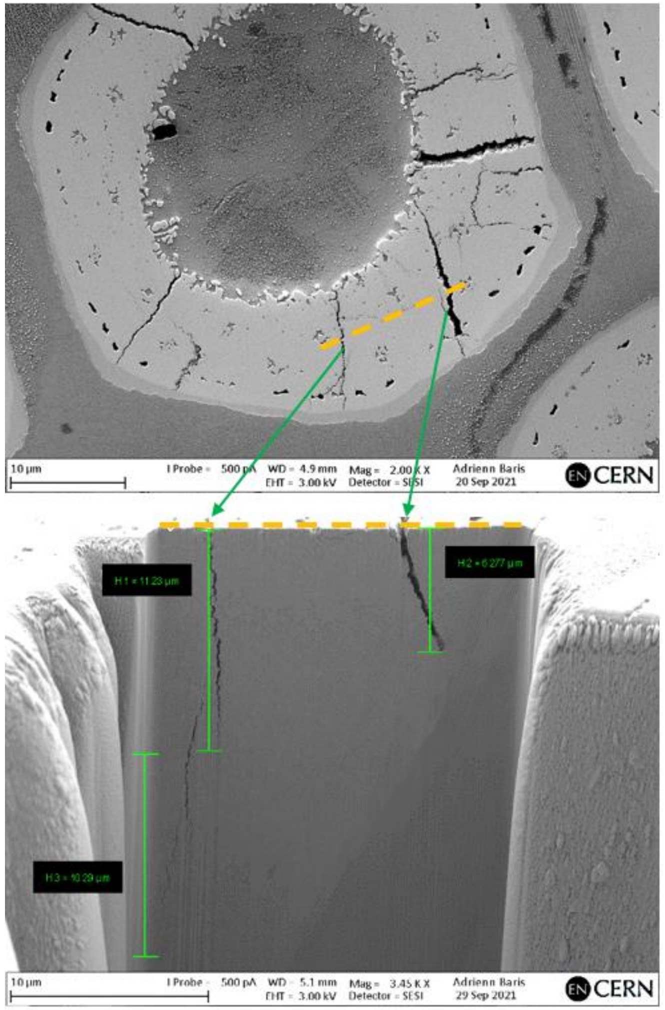

- Example **of crack propagation** within a fractured sub–element in the connection-side head of 11 T dipole magnet coil C122 (not used in a magnet).
- **Top:** top view of a sub–element showing **superficial radial cracks** in the aggregate of reacted filaments; the orange dashed line represents the removal plane of the **Focused Ion Beam (FIB).**
- **Bottom: crack propagation along the sub–element axis;** green arrows point to the corresponding superficial cracks, while the orange dashed line corresponds to the one of the top image (note that a third sub–superficial crack is also observed).

Courtesy of A. Baris
(CERN/EN-MME)

From ITER to HL-LHC…

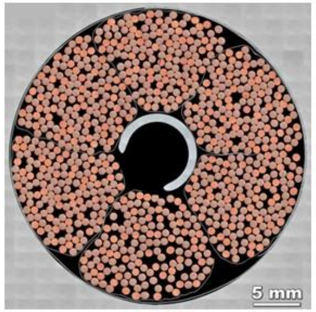

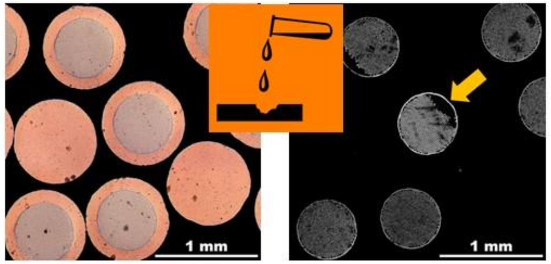

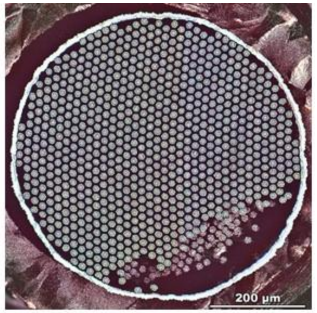

Courtesy of P. Lee (FSU)

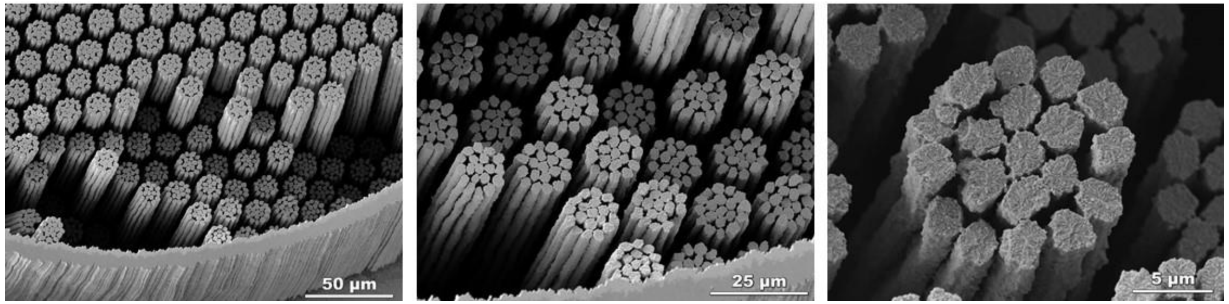

ITER 2010s

- In the case of ITER CICC, the **root cause** of degradation was attributed to **strand bending.**

- *Most heartfelt thanks to Peter Lee, Matt Jewell and Charly Sanabria for their* ***pioneering imaging work,*** *which has been an inspiration and a model.*

- **Different conductor** (cable-in-conduit conductor with direct, forced-flow helium cooling vs. resin-impregnated, Rutherford-type cable), but **similar phenomenology.**

HL-LHC 2020s

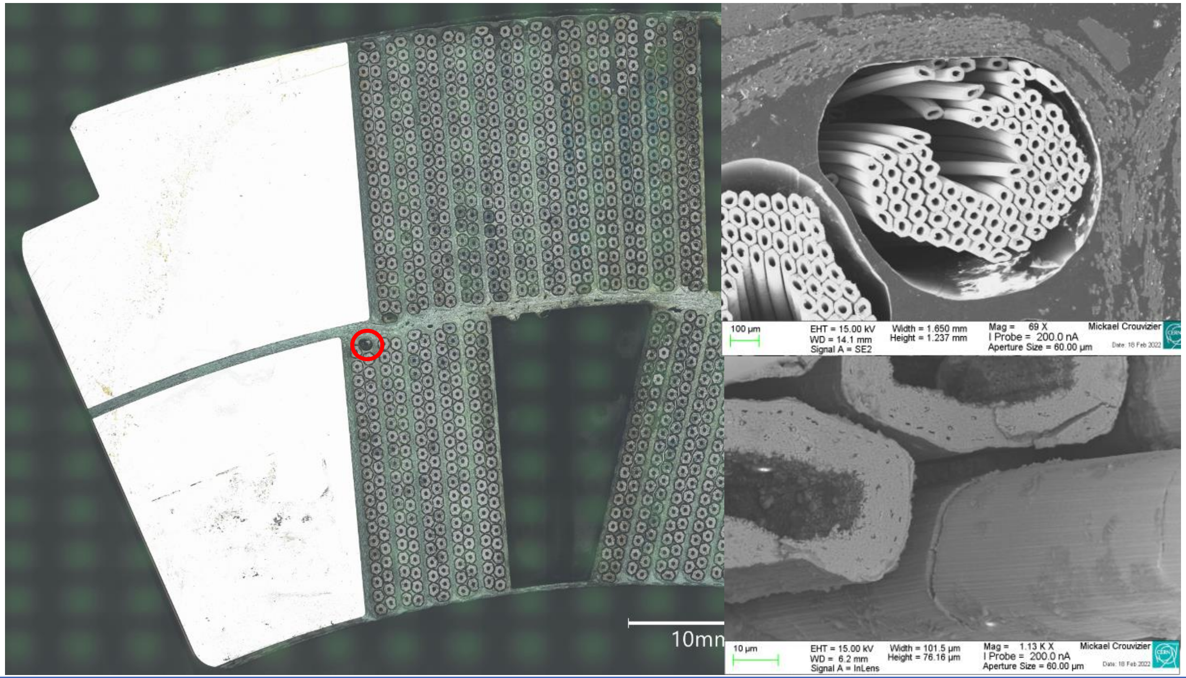

Recovery Plan for HL-LHC MQXFB Quadrupole Magnets @CERN

Root-Cause Analysis

Recovery Plan for MQXFB

Root-Cause Analysis for MQXFB @CERN

- Following the **limitation** observed on the first two **MQXFBP1&2** prototypes **below nominal current at 1.9 K,** a thorough analysis was carried out and **three possible root causes** were identified

  (1) cold mass assembly: non-optimum **mechanical coupling** between welded outer stainless steel and magnet structure (aluminum rings).

  (2) magnet loading**:** non-optimum **magnet assembly parameters and processes** (*e.g.*, during bladdering and keying) leading to unbalanced and/or excessive coil peak stresses;

  (3) coil manufacturing**:** issues during **coil manufacturing and/or handling** leading to coil non-uniformities and/or deformation.

- Of course, it could be a **combination of the three,** or there could be **one predominant cause,** and the others may **exacerbate the problem.**

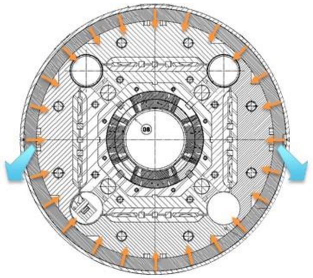

Initial MQXFB cold mass design with **tight mechanical coupling** between outer shell and magnet structure (*à la* LHC)

Courtesy of H. Prin (CERN/TE-MSC)

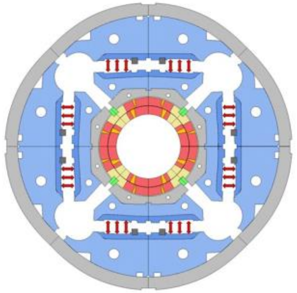

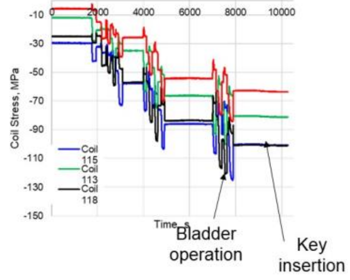

Initial MQXFB loading procedure with significant **coil stress overshoot** at time of bladdering

Courtesy of J. Ferradas Troitino and S. Izquierdo Bermudez (CERN/TE-MSC)

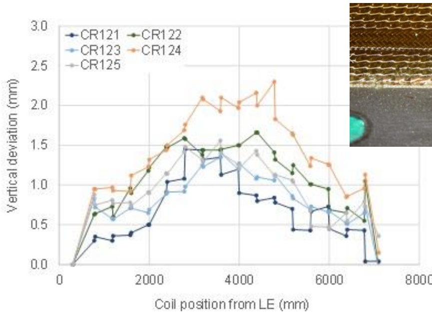

"Hump" after HT

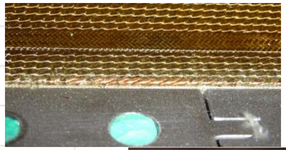

Protrusion of inner pole turn

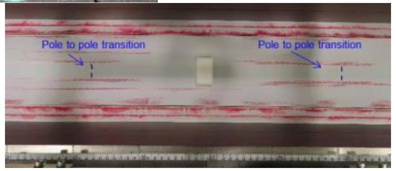

Fuji paper test on CR126

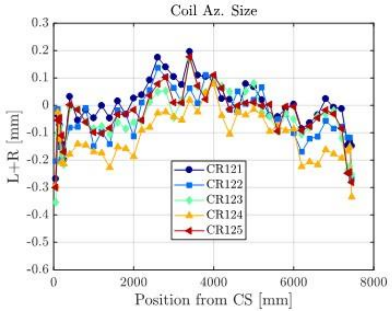

"Belly" after VPI

Observations of coil hump and conductor protrusion after HT, stress concentration at **Ti-pole junctions** upon closure closure of VPI mold, and coil belly after VPI

Courtesy of N. Lusa and A. Milanese (CERN/TE-MSC)

Recovery Plan for MQXFB @CERN (1/4)

- Due to **manufacturing lead times,** the three root causes could only be addressed in **"reverse order"** (shell welding, then magnet assembly, then coil manufacturing); however the results of each stage were fed back into the subsequent one.

- ***First stage:*** ***cold mass assembly***
  - Already assembled cold mass **MQXFB01** was dismounted and reassembled into **MQXFBP3** with **re-optimized shell design** and **welding parameters;**
  - The re-optimization consisted in increasing the **shell developed length** and in ensuring that the **weld shrinkage** would not result in **radial interference** between shell and magnet structure;
  - The redesign required the implementation of a **fixed point** between **outer shell and magnet structure;**
  - **MQXFBP3** was tested in **Q2/Q3 2022;** it achieved **target current at 1.9 K,** but exhibited a **limitation at 4.5 K,** with the same phenomenology as for MQXFBP1&2, but at a higher current level.

Courtesy of H. Prin
(CERN/TE-MSC)

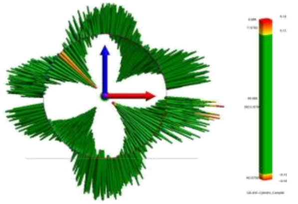

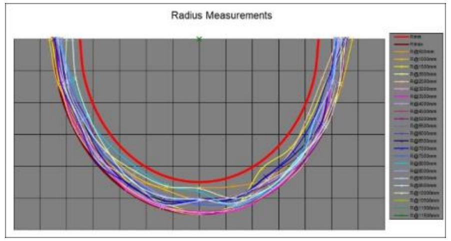

Optimization of outer shell developed length on MQXFB

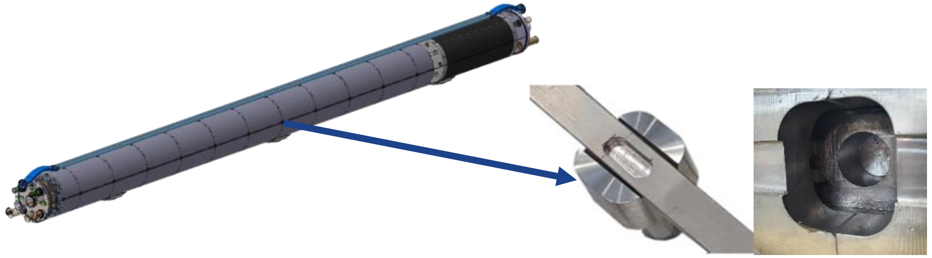

Fixed point implementation on MQXFB (to sustain 10-bar pressure wave corresponding to ~235 kN force)

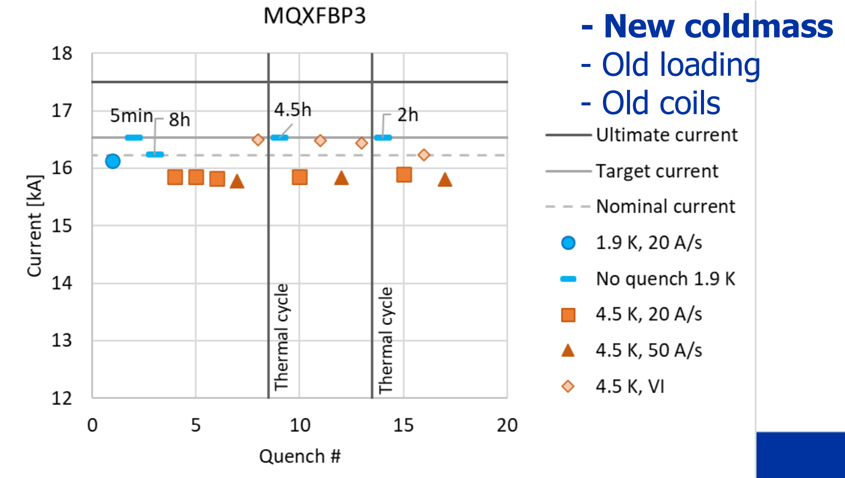

Quench performance of MQXFBP3

Recovery Plan for MQXFB @CERN (2/4)

- ***Second stage: magnet loading***

  – **Magnet loading procedure** was improved by implementing **additional bladders** into yoke cooling holes, which enable to **stretch iron yoke and aluminum rings outwardly** rather than push inwardly onto the collared coils;

  – New procedure **successfully validated** on a full-length mechanical model **MQXFBMT3** assembled in **Q1 2022** with Fuji paper up to full force**; stress overshoot** observed on all previous magnet loadings was **eliminated.**

  – **MQXFB02** was assembled with **optimized bladdering/ keying parameters,** using already manufactured (virgin) coils and optimized shell welding qualified on **MQXFBP3;** it was first tested in **Q4 2022** and endurance-tested in **Q1 2023.**

  – Similarly to **MQXFBP3, MQXFB02** achieved **target current at 1.9 K,** but exhibited a **limitation at 4.5 K,** with the same phenomenology, but, again, at a slightly higher current level.

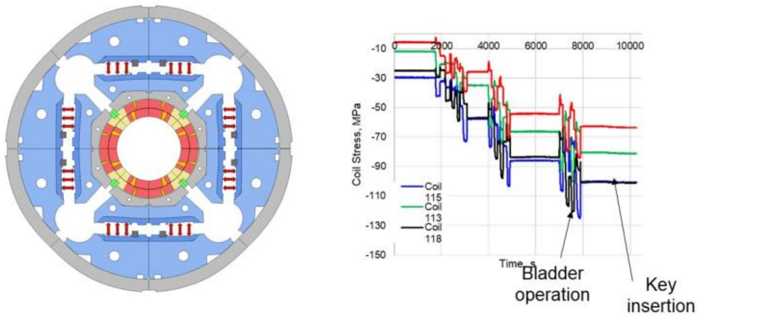

Initial MQXFB loading procedure with significant coil stress overshoot at time of bladdering

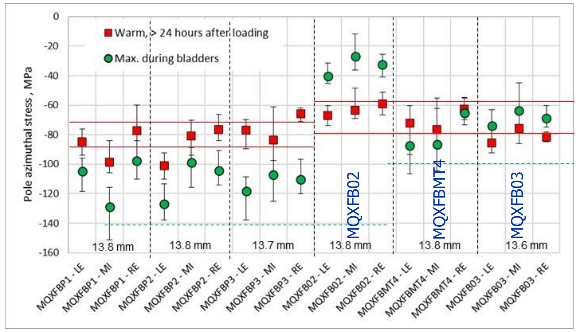

Loading history of 7.2-m-long MQXFB magnets

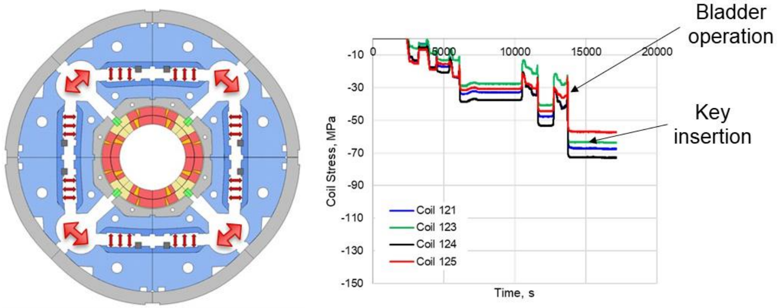

Optimized MQXFB loading procedure with no coil stress overshoot

Courtesy of J. Ferradas Troitino and S. Izquierdo Bermudez (CERN/TE-MSC)

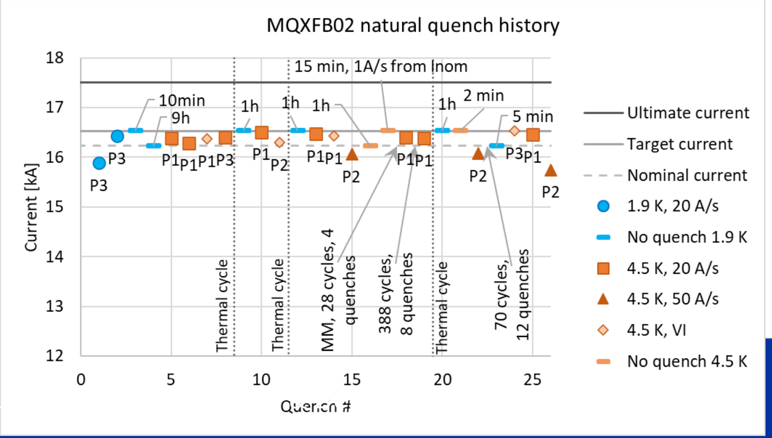

- **New coldmass**
- **New loading**
- Old coils

Recovery Plan for MQXFB @CERN (3/4)

- Stage-1 and -2 recovery actions enabled **MQXFBP3** and **MQXFB02** to **reach and hold nominal current + 300 A at 1.9 K for several hours,** but they still exhibited **performance limitation at 4.5 K,** similar to that of first prototypes, but at **progressively higher levels.**

- The first **two recovery actions were beneficial,** but the **root cause had not yet been fully eradicated;** decision was taken to proceed with **3rd recovery action.**

- ***Third stage: coil manufacturing***

– **3 transition coils** were manufactured **(127, 128, 129)** aiming at **reducing/eliminating hump and belly** at coil centers, and the **hinge effect** that may occur on pole turn conductors in the vicinity of the **Ti-pole junctions** at the time of HT mold opening and VPI mold closure.

– Goal was achieved on **coils 128 & 129,** thanks to changes in process parameters (*e.g.*, **removal of ceramic binder** on coil outer layer); decision was taken to manufacture coils of next magnet **(MQXFB03)** with such processes; tested **in Q3/Q4 2023**.

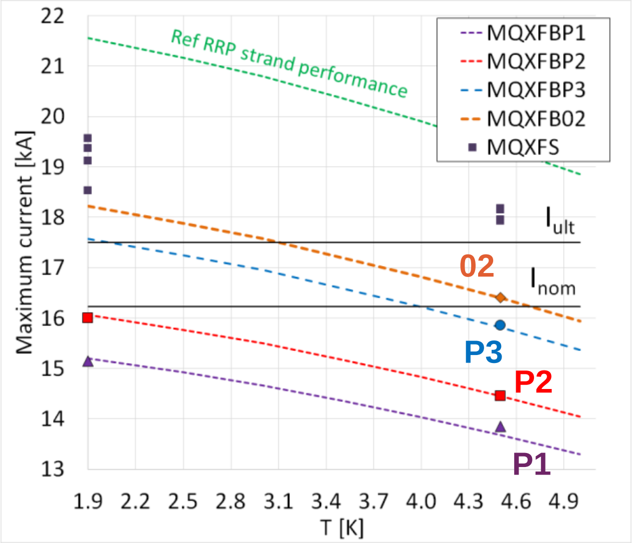

Quench current vs. temperature of full-length MQXFB magnets exhibiting performance limitation at 4.4 K

Ceramic binder application by brushing

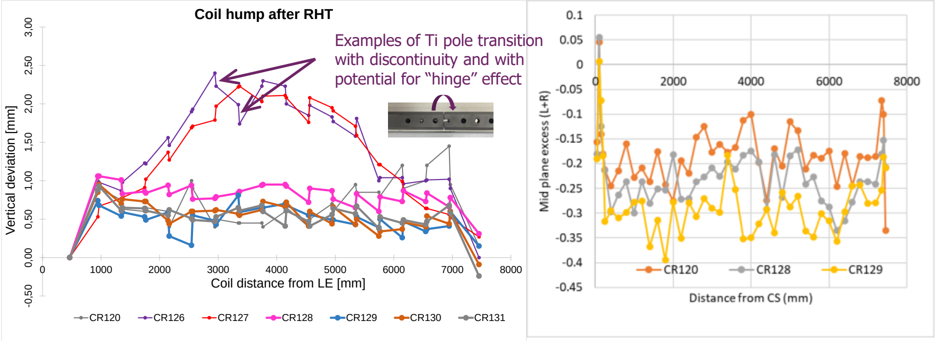

Elimination of coil hump & belly starting from coil 128

Significant reduction of protrusion effect at Ti pole junctions

Courtesy of
S. Izquierdo Bermudez, N. Lusa and A. Milanese
(CERN/TE-MSC)

Recovery Plan for MQXFB @CERN (4/4)

- **MQXFB03** is the **3rd magnet of 3-stage strategy,** integrating all recovery actions
  - **(1) improved** ***cold mass assembly*** and fixed point;
  - **(2) improved** ***magnet loading*** to avoid overshoot;
  - **(3) improved** ***coil manufacturing*** to remove hump & belly.
- It was tested in **Q3/Q4 2023** and is the first 7.2-m-long MQXFB magnet to **achieve target current of 16.53 kA** at both **1.9 K and 4.5 K.**
- It shows **good endurance** after **2 warm-up/ cooldown cycles** with no retraining at 1.9 K; **no ramp rate degradation** up to **100 A/s;** initial **training quenches at 1.9 K** are all in **coil ends** (2 training quenches at 4.5 K upon reaching target current plateau under investigation).
- **Performance limitation** and **phenomenology** observed on previous, full-length, MQXFB magnet straight sections (near apex of hump & belly) have been **overcome** and **root cause** has been **eliminated.**
- **Series production** has been **launched;** next magnet was tested in **Q2 2024.**

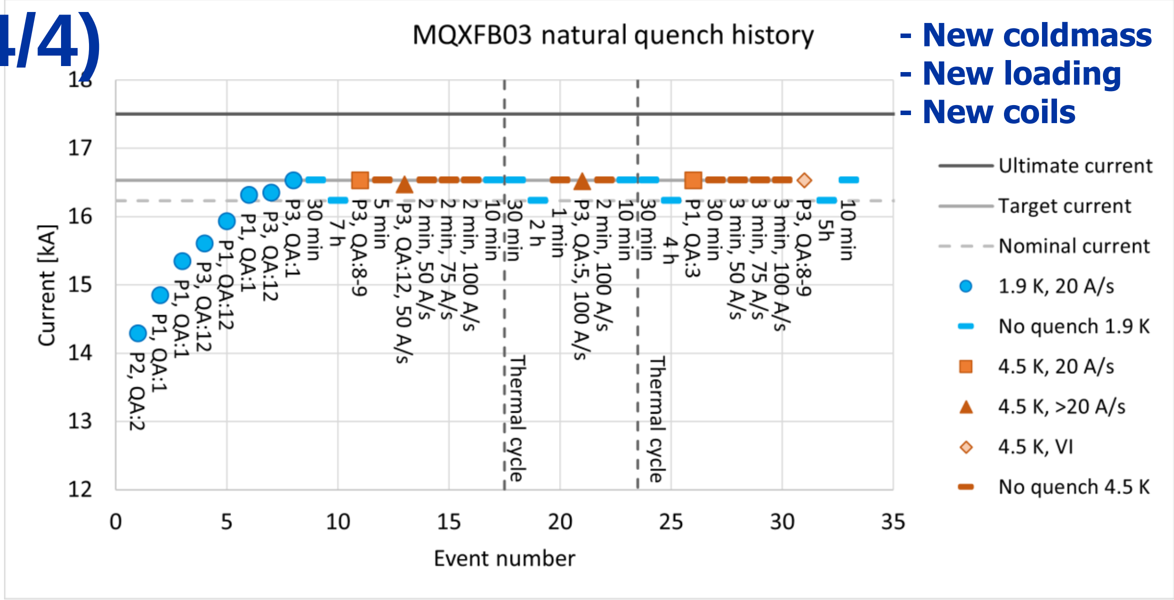

Quench Performance of 7.2-m-Long MQXFB03 Quadrupole Magnet at CERN

Courtesy of F. Mangiarotti (CERN/TE-MSC)

Ramp rate sensitivity of 7.2-m-Long Quadrupole Magnets at CERN

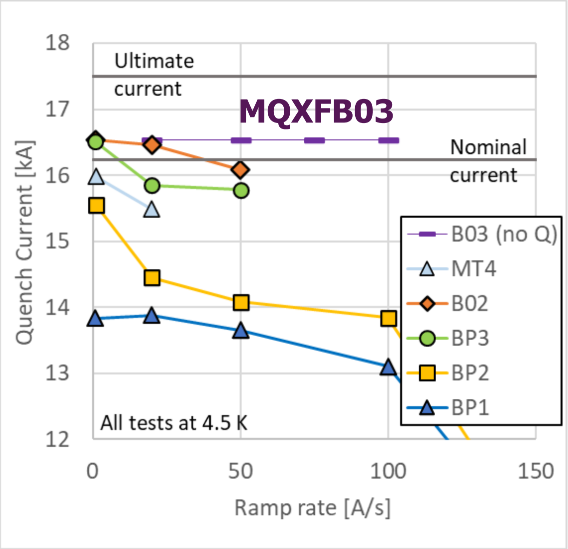

MQXFB @CERN (Cont.)

- **MQXFB04** is the **1st virgin MQXFB magnet** assembled with a **MCBXFB nested corrector** in a **final Q2 cold mass & cryostat** configuration.
- It is the **2nd MQXFB magnet** (after **MQXFB03)** integrating all **3 recovery actions;** test with **2 cooldowns** carried out in **April & May 2024.**
- **Three training quenches** to reach **target current @1.9 K** after **1st cooldown.**
- **One training quench** above nominal current to reach **target current @1.9 K** after **2nd cooldown.**
- Reached **nominal current @4.5 K** after **both coooldowns;** reached **target current @4.5 K** after **2nd cooldown.**
- **No measurable voltage** during ***V-I* measurements @4.5 K.**
- **MCBXFB corrector magnet** successfully tested **without quench.**

Q2 Cryomagnet with MQXFB04 coldmass on SM18 Test Bench

Courtesy of F. Mangiarotti
(CERN/TE-MSC)

- Final Q2 configuration
- New coldmass
- New loading
- New coils

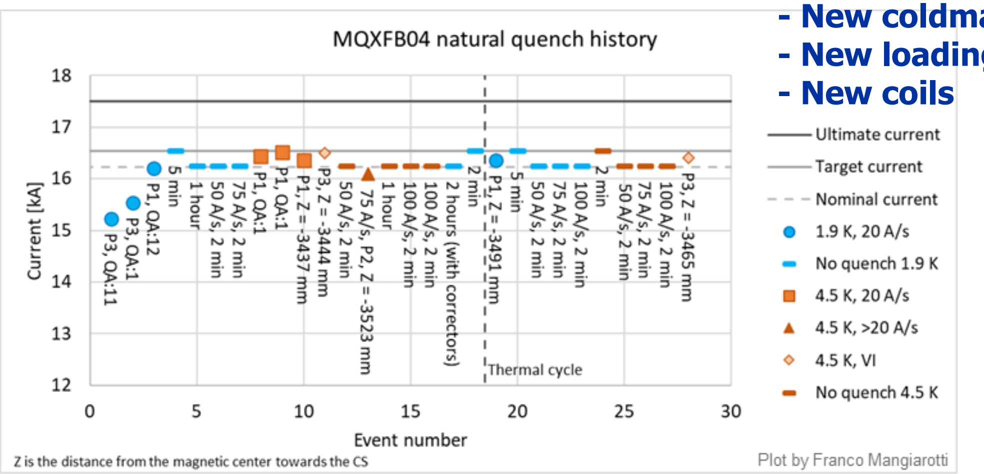

Quench Performance of 7.2-m-Long MQXFB04 Quadrupole Magnet at CERN

From ITER to HL-LHC… (Cont.)

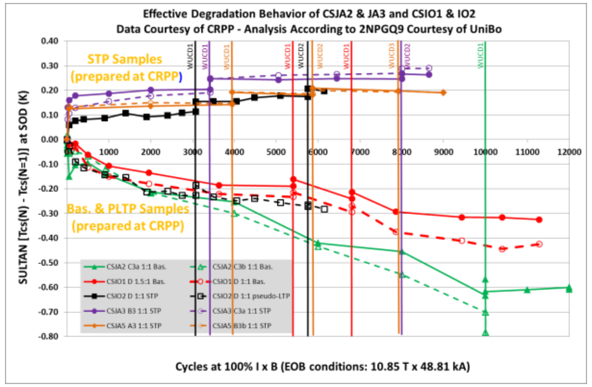

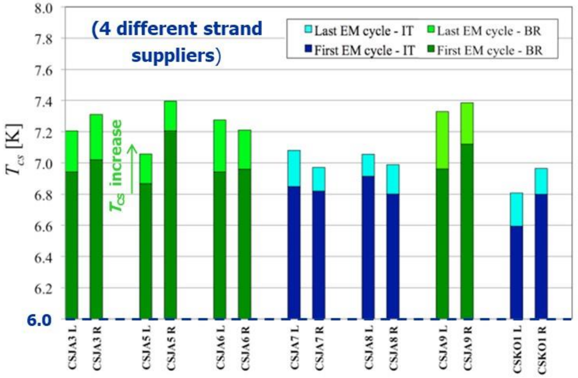

Courtesy of M. Breschi & D. Macioce (UniBo)

Short-twist-pitch cabling pattern for ITER CS
Courtesy of C. Sanabria (formerly FSU)

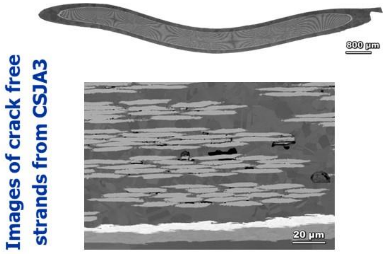

ITER 2010s

- **Root cause of performance limitation of MQXFB magnets** was resolved by controlling **Nb_3Sn coil uniformity and deformation** during manufacturing process and preventing subsequent **coil overstressing.**

- Performance degradation of ITER CICCs was resolved by changing **cabling pattern** to **short-twist-pitch** preventing **Nb_3Sn strand bending during energization.**

- **Post-mortem metallographic analyses** confirmed **absence of cracks.**

HL-LHC 2020s

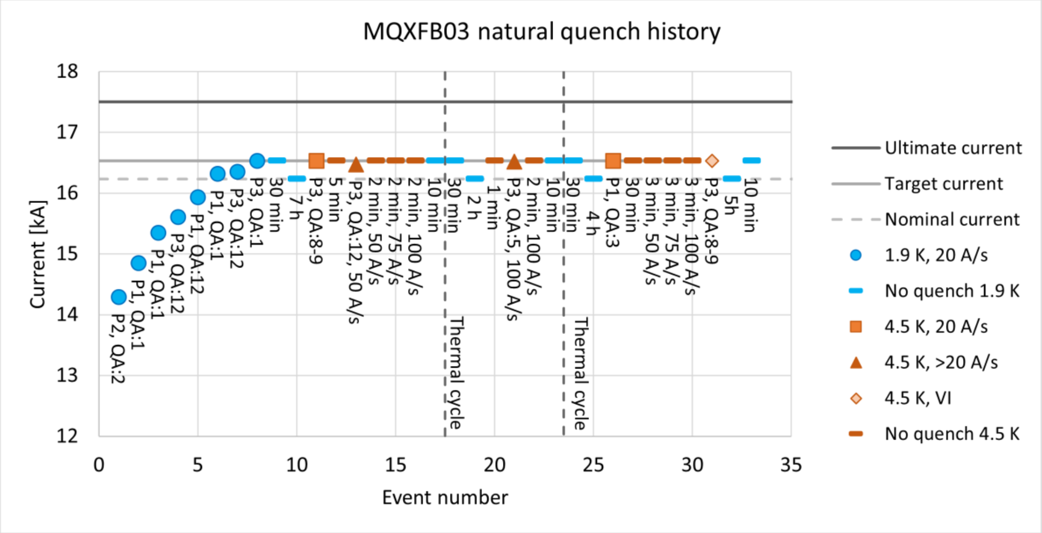

Highlights on MQXFA (US Contribution)

- **AUP** has completed the assembly and has successfully tested on a horizontal bench at Fermilab the first **Q1/Q3 cryo-magnet (LQXFA01).**
- **LQXFA01** includes 2 x 4.2-m-long quadrupole magnets: MQXFA03 and MQXFA04, which were previously tested in vertical station; neither of them exhibited **any retraining.**
- **LQXFA01** was **shipped to CERN** and arrived in SMI2 on 28 November 2023.
- It will be retested at CERN on **upgraded test bench A2** in June 2024 prior to installation in the string (but cannot be used as is for tunnel installation).
- **AUP** has also completed the vertical test of MQXFA15 at BNL with **very good training performance.**

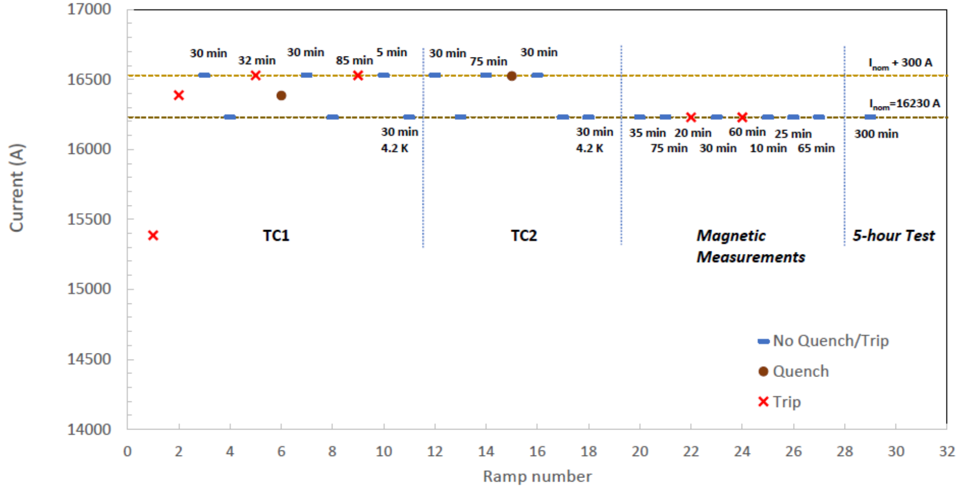

Quench summary of LQXFA01 tested horizontally at Fermilab

Courtesy of S. Feher and G. Ambrosio (Fermilab)

First AUP LQXFA01 cryomagnet mounted on Cryostat Tooling in SMI2 at CERN

Courtesy of D. Duarte Ramos (CERN TE-MSC)

Diversification Projects @CERN, *e.g.*

Strongly-Curved, Nb–Ti, CCT Demonstrator

Energy-Efficient, MgB_2, Superferric Dipole

Strongly-Curved, Nb–Ti, CCT Demonstrator (Fusillo; 1/3)

- Emerging applications call for the development of **strongly-curved, moderate field, Nb–Ti, multipolar magnets,** for which **Canted Cosine-Theta (CCT)** design shows promising potentials.
- **Fusillo** is a **dipole magnet demonstrator,** with bore/peak fields of **3.00/3.56 T** in a **230-mm** aperture bent over **90° with a 1-m radius,** and is aimed at exploring these potentials.
- The project was initiated by **G. Kirby,** iterated by **D. Tommasini** and taken over by **A. Haziot** as part of a (successful) succession plan.
- It capitalizes on the **HL-LHC MCBRD development,** at CERN and extends the development carried out at **LBNL** in 2019, which produced a magnet model with a central field of **2.4 T** in a **290-mm** aperture bent over **45° with a 0.9 m radius.**
- Possible applications are: bending magnets for **Isolde Superconducting Recoil Separator (ISRS)** at CERN or for **compact ion therapy gantry** systems.

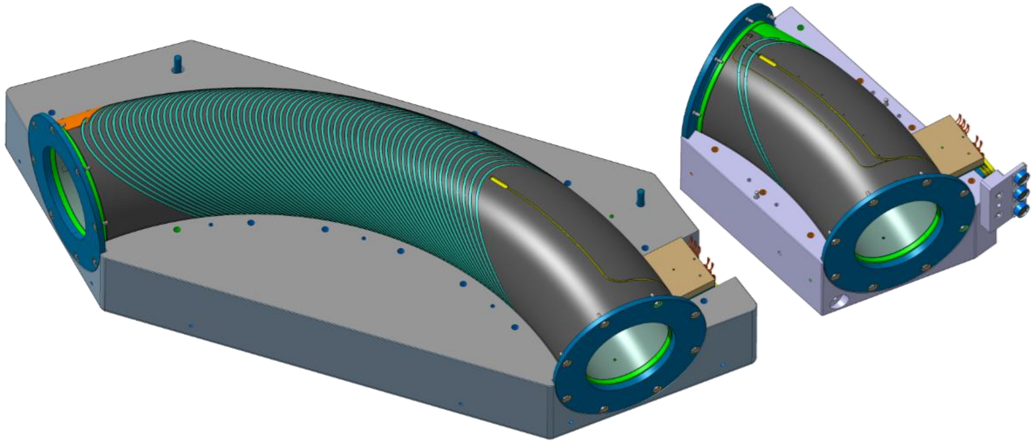

3D-CAD Models of subscale model and full-scale fusillo demonstrator at CERN

Courtesy of A. Haziot
(CERN/TE-MSC)

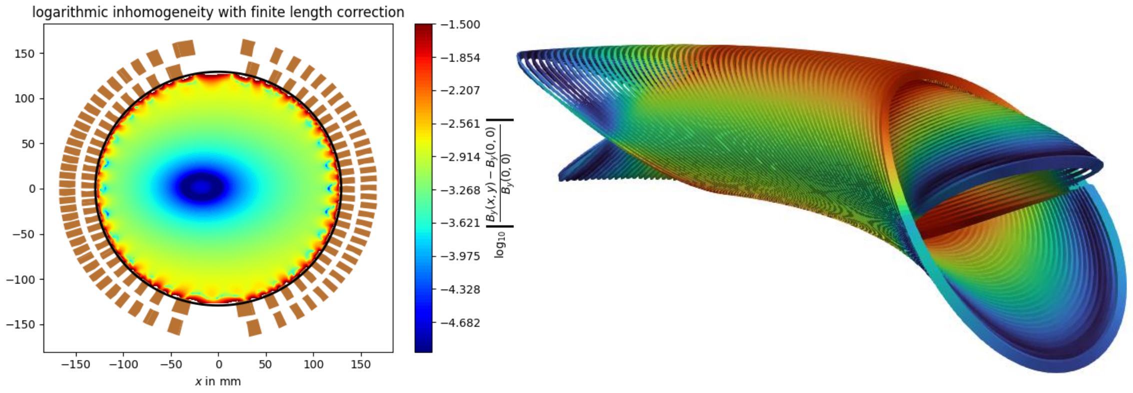

Field Maps of Full-Scale Fusillo Demonstrator (generated by Roxie)

Strongly-Curved, Nb–Ti, CCT Demonstrator (Fusillo; 2/3)

- Several **improvements/innovations** are under consideration for Fusillo
  - **Enhanced** electromagnetic modelling;
  - 6-around-1 cable;
  - Improved **polyimide insulation** and resin system;
  - Improved connection box and **splicing technique;**
  - **Machining and assembly** of formers.
- Innovations are qualified in **sub-scale models** with same aperture, same radius, same forces, same margin on load line, but 1/3rd of the length.
- **2 sub-scale models** have been completed and tested at 4.5 K **(**first one in August 2023, second one in March 2024).
- Both exceeded **nominal current without** and reached quench near short sample limit.
- **Magnetic measurements** are in good agreement with Roxie simulated data.

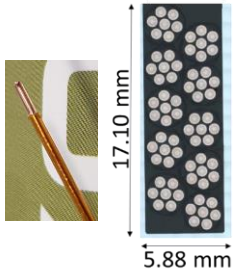

Insulated Fusillo wire and X-sectional view of Fusillo winding

Winding of sub-scale Fusillo model

Assembly of sub-scale Fusillo model

Courtesy of A. Haziot (CERN/TE-MSC)

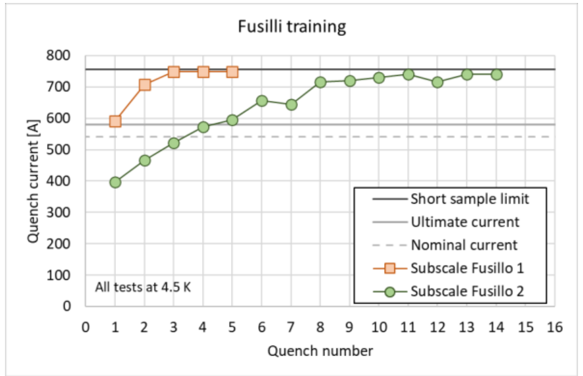

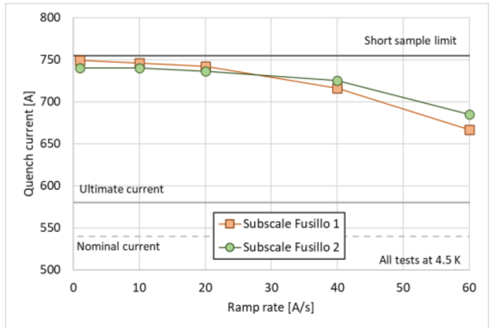

Courtesy of F. Mangiarotti (CERN/TE-MSC)

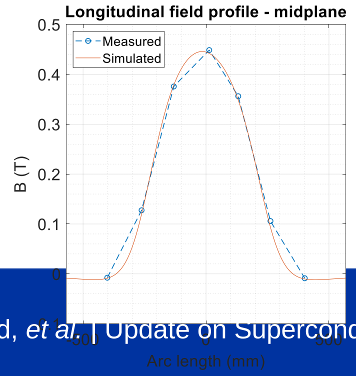

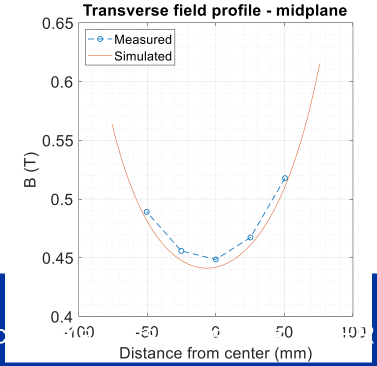

Courtesy of C. Petrone (CERN/TE-MSC)

Strongly-Curved, Nb–Ti, CCT Demonstrator (Fusillo; 3/3)

- **Manufacturing of components** of **full-scale** components is proceeding.
- **New winding machine** has been procured and installed at CERN (Bldg. 927); **now under commissioning.**
- **Winding** to start in **June 2024**, **impregnation** in **July 2024** and **cold test** in **September 2024.**

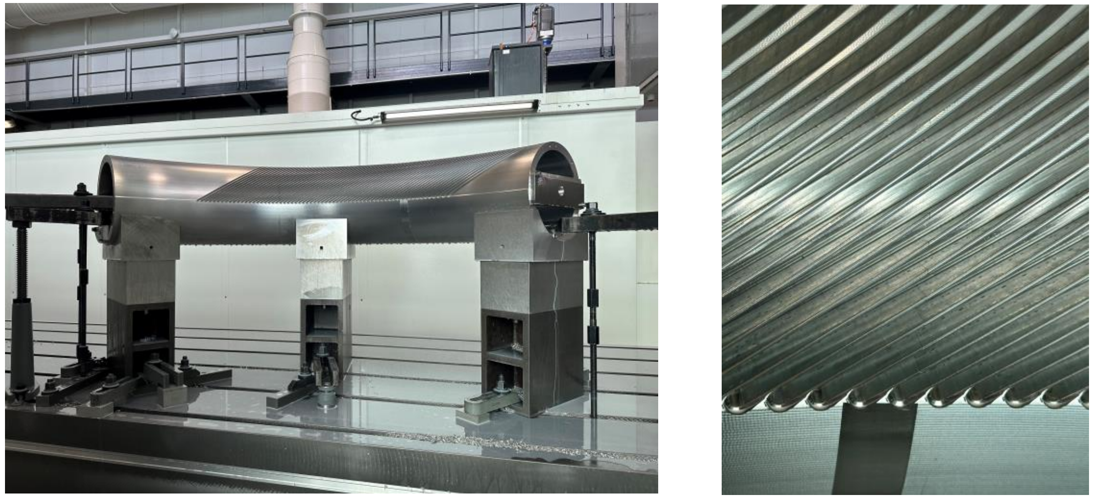

Machining of 3-part inner mandrel is completed

Commissioning of new winding machine is underway at CERN

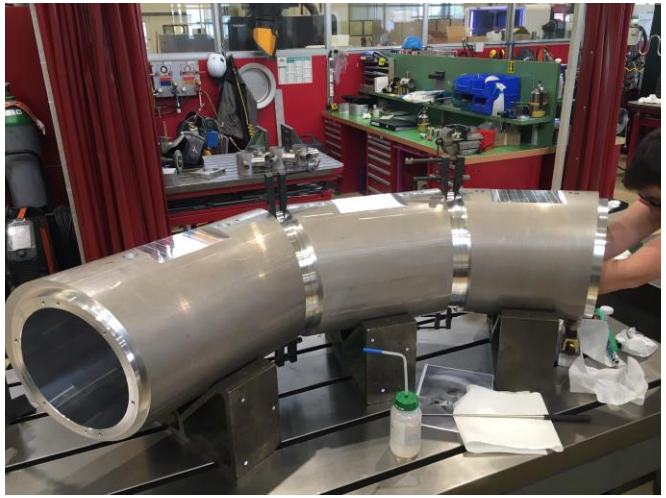

Assembly of 3-part outer mandrel is completed

Courtesy of A. Haziot
(CERN/TE-MSC)

Energy-Efficient Superferric Dipole (1/3)

- A number of physics experiments call for the use of **iron-dominated, normal-conducting electromagnets** to produce **moderate fields (2 T range)** in a large gap or large volume; although robust and reliable, these magnets require **significant electrical power** –in the MW range– and can be costly to operate, especially in DC mode.
- The EESD program is aimed at exploring the potential of a **superferric magnet design** based on one of the **MgB_2 cables** developed as part of HL-LHC WP6a and operated in **gaseous helium (Ghe) at 20 K.**
- First step, is a **proof-of-principle demonstrator** whose design and assembly processes are **representative** and can be easily **scaled up** to large, iron-dominated magnets for physics experiments; main design parameters are
  - **H-type** iron yoke;
  - Single, double-pancake, **racetrack-type** coil;
  - Pole gap: **180 x 62 mm;**
  - Magnetic length: **1.0 m;**
  - Target central field: **1.8–2.0 T at 5 kA** (coil peak field ≤ **1.1 T).**

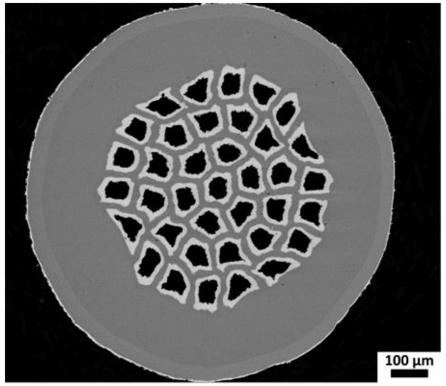

MgB_2 wire for HL-LHC superconducting link

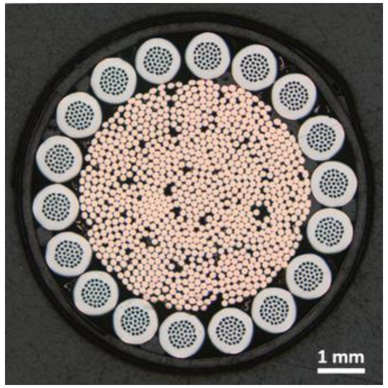

MgB_2 cable (18 MgB_2 strands twisted around braided copper core)

Courtesy of A. Ballarino
(CERN/TE-MSC)

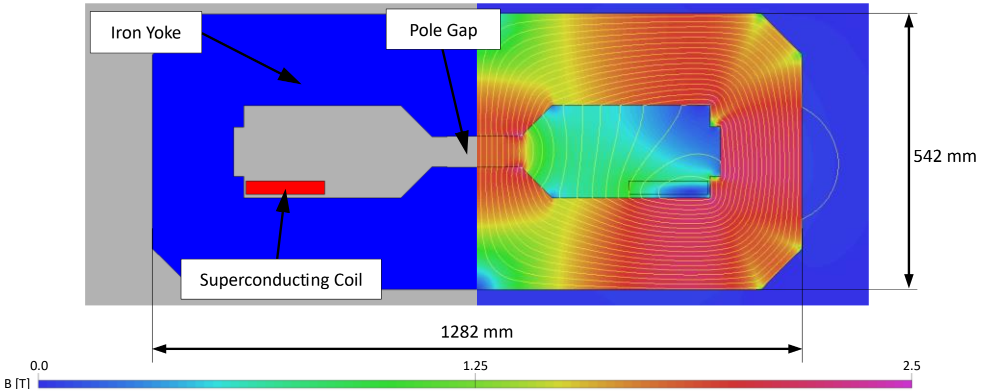

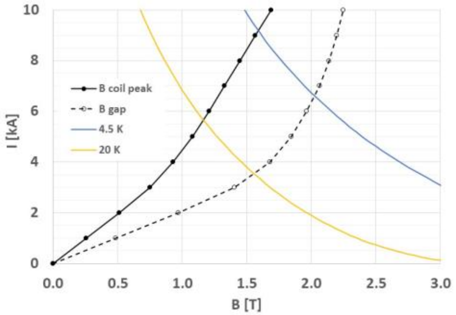

2-D electromagnetic design and magnet load lines with reference MgB_2 cable data at 4.5 K and 20 K

Courtesy of A. Milanese
(CERN/TE-MSC)

Energy-Efficient Superferric Dipole (2/3)

- **Double-pancake coil** is wound, without tension, positioning the cable in half circular grooves of **aluminum alloy (grade 6082) formers;** grooves are machined precisely to obtain a tight fit with insulated cable, thus supporting it during powering (à la **ITER TF radial plates).**
- Test of Proof-of-Principle demonstrator is planned in **three phases**

  (1) test in a cryogenic test station with **LHe at 4.5 K;**

  (2) test in a cryogenic test station with **GHe at 20 K;**

  (3) test with **warm iron** and **coil at 20 K** in a dedicated cryostat.
- **Phase 1** tests were successfully carried out in **Summer of 2023:** demonstrator was powered up to **5 kA without quench nor *V-I*** and was subjected to a thermal cycle to room temperature.
- **Magnetic measurements** were performed with rotating coil magnetometer and are consistent with FE simulations: measured central field is **1.95 T at 5 kA.**

EESD team

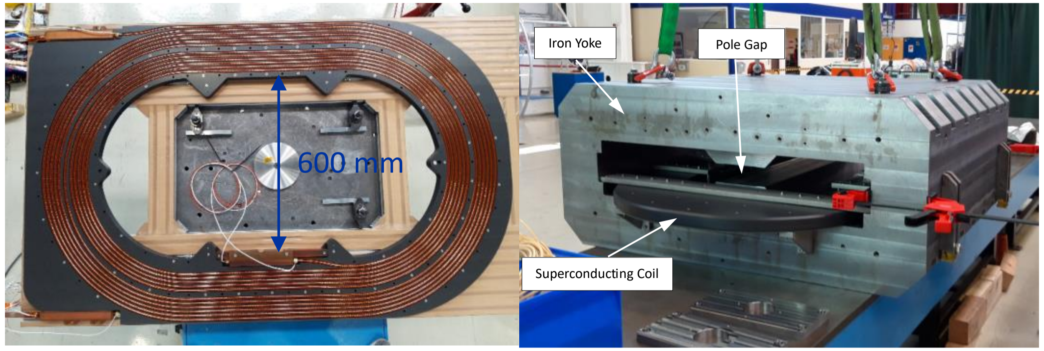

Assembly of proof-of-principle EESD demonstrator

Courtesy of N. Bourcey and A. Milanese (CERN/TE-MSC)

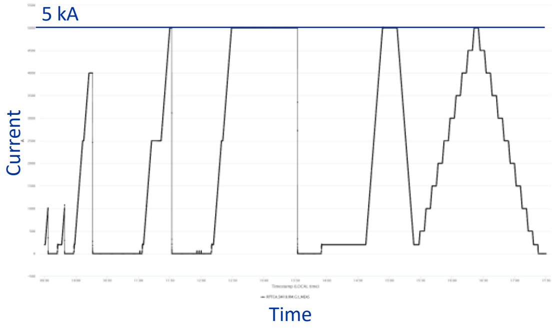

EESD powering history during first test cycle at 4.5 K (Phase 1).

Courtesy of F. Mangiarotti (CERN/TE-MSC)

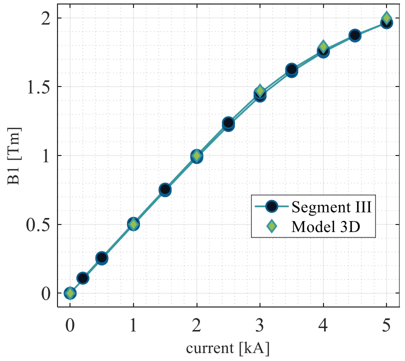

Integral dipole field load line

Courtesy of C. Petrone (CERN/TE-MSC)

Energy-Efficient Superferric Dipole (3/3)

- **Phase 2** tests started **this week:**
  - Demonstrator was first cooled down to **4.5 K** to re-establish **previously achieved performances;**
  - Demonstrator was then warmed up to **20 K** and successfully powered up to **4 kA without quench nor *V-I.***
- **Next steps** are tests at **higher temperatures (25** and **30 K).**
- **Cryostat design** for **Phase 3** is underway.

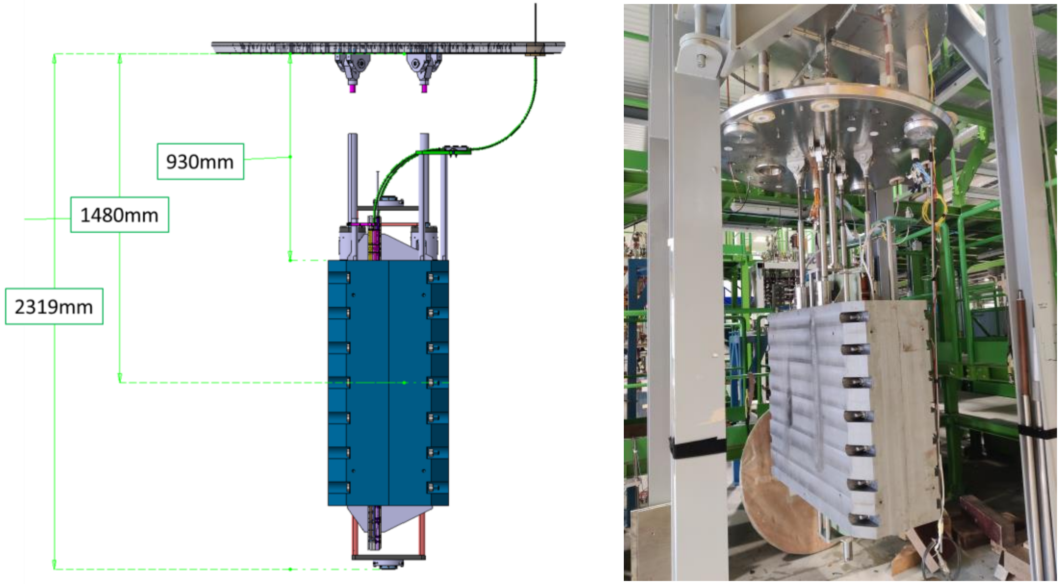

Reassembly of EESD demonstrator for Phase 2

Courtesy of N. Bourcey and A. Milanese (CERN/TE-MSC)

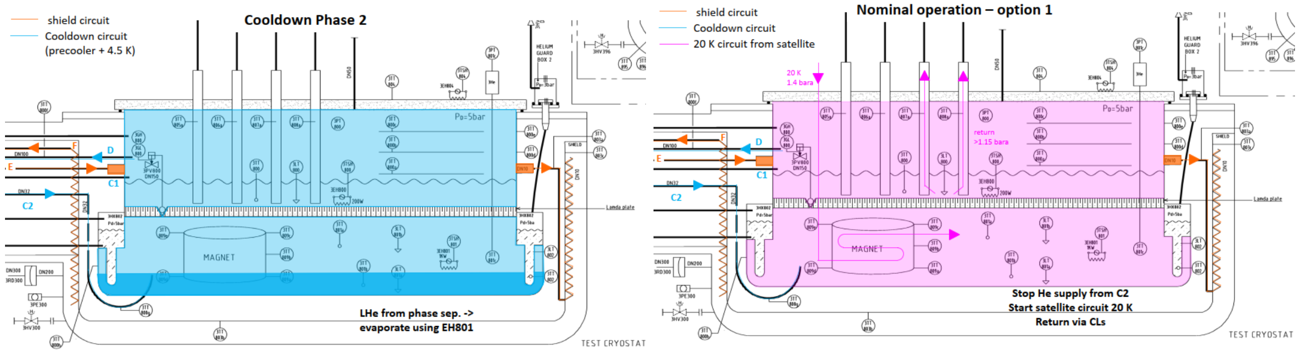

PIDs for cooldown and 20-K operation

Courtesy of P. Tavares (CERN/TE-CRG)

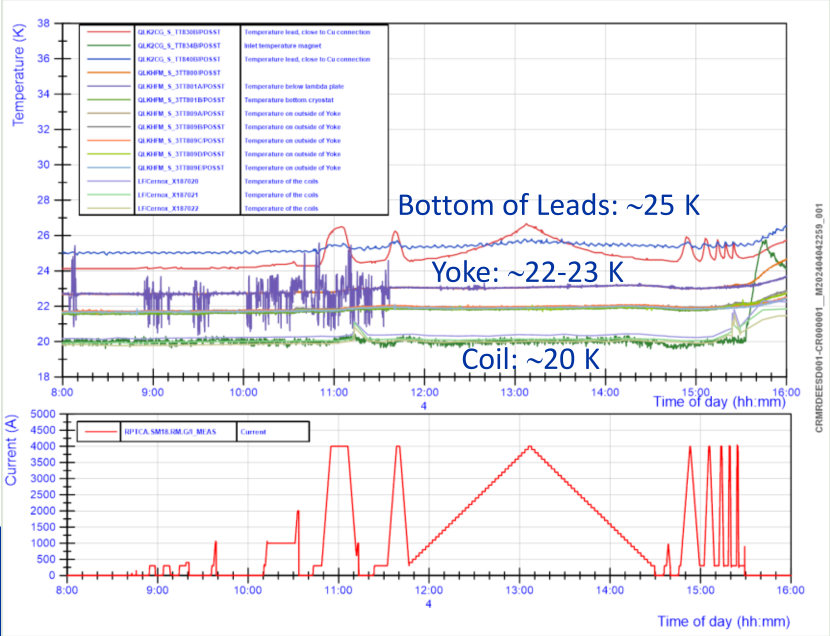

EESD powering history during first test cycles at 20 K (Phase 2).

Courtesy of G. Willering (CERN/TE-MSC)

Conclusion

Conclusion

- **HL-LHC** will see the first large-scale application of **MgB_2 superconducting links** **and** **Nb_3Sn accelerator magnets**.

- **The superconducting link** concepts and technologies have been validated through a **prototype system test;** cold results (including one **warm-up cooldown cycle)** are **excellent:** system was able to transport up to **94 kA** with **5 g/s GHe flow;** it will be subsequently installed in the **integrated string test** foreseen at CERN in **2025/2026.**

- CERN has overcome the **performance limitation** encountered on the **7.2-m-long, Nb_3Sn quadrupole magnets** and has tested two full-size magnets that have reached target current at both **1.9 K and 4.5 K;** it can now proceed (alongside AUP) with the **small series production** needed for HL-LHC.

- **Nb_3Sn** has been demonstrated to be a **viable and robust technology** for **fusion** and **accelerator** magnet applications, and is now reaching **maturity,** thanks to **ITER** and **HL-LHC;** there is **no inherent issues** with the technology, but it requires reliance on **good engineering practices** for **cabling, coil manufacturing** and **magnet/cold mass assembly.**

- **The technologies developed for HL-LHC** enable the emergence of new applications (*e.g.*, **strongly-curved, CCT magnets** and **energy-efficient superferric magnets),** which may have **positive societal impacts.**

home.cern

Abstract

Update on Superconducting Magnets & Devices Development at CERN.

The High Luminosity LHC (HL-LHC) project at CERN has offered the opportunity to promote and develop various types of enabling accelerator technologies, such as MgB2 superconducting links for cold powering and Nb3Sn accelerators magnets for the interaction regions. The superconducting link is in an advanced prototyping phase and is expected to be fully validated in the coming months. The Nb3Sn magnet development has encountered serious difficulties characterized by performance limitation or degradation which have now been overcome. We report on the status and challenges of HL-LHC magnets and devices at CERN, with a primary focus on the root cause analysis and recovery actions implemented for the final focusing Nb3Sn quadrupole magnets, and a comparison with similar issues encountered over a decade ago on the Nb3Sn Cable-in-Conduit conductors for ITER magnets. We also present two ongoing spin-off projects which benefit from HL-LHC technology developments: a strongly curved, Nb-Ti, canted cosine theta (CCT) magnet and an energy-efficient, MgB2, superferric dipole magnet.

Biography

After a PhD in Applied Superconductivity at CEA/Saclay, France, Arnaud Devred joined the Central Design Group of the Superconducting Super Collider (SSC) in Berkeley, CA in December 1987 where he worked on test and analysis of dipole magnet prototypes. In September 1989, he moved to KEK High Energy Accelerator Research Organization, in Tsukuba, Japan as part of the team who manufactured the 1st 5-cm-aperture, SSC dipole magnet model, and, in September 1990, joined the SSC Laboratory to lead the Magnet Science Section. In 1994, he came back to CEA/Saclay, where he became Head of the Magnetic Measurement Laboratory and initiated a Nb_3Sn accelerator magnet program. In 2004, he set up the first collaboration of European institutes to work on a Joint Research Activity named the Next European Dipole (NED). Throughout that period, he also held various associated positions with CERN, in Geneva, Switzerland, where he provided advices on the design and production of superconducting magnets for the Large Hadron Collider (LHC). In August 2007, he was recruited to lead the Superconducting Systems & Auxiliaries Section at the ITER International Organization, in Cadarache, France, where, among others, he oversaw the in-kind procurement of the Cable-in-Conduit conductors for the ITER magnet system. Once the ITER conductor procurement was nearly completed, he joined CERN where he eventually became Leader of the Magnets, Superconductors and Cryostats Group, in charge, in particular, of the magnets for the High Luminosity upgrade of the LHC (HL-LHC). Following the success of recent 7.2-m-long Nb_3Sn quadrupole magnets for HL-LHC, he has been appointed in January 2024 Senior Advisor to the CERN Technology Department. Arnaud Devred is the recipient of a 2014 Award for Continuing and Significant Contributions in the Field of Applied Superconductivity of the IEEE Council on Superconductivity.